

Pictorial Representation for Antisymmetric Eigenfunctions of $PS-3$ Integral Equations

Andrei Borisovich Bogatyrev

Received: 27 March 2008 / Accepted: 15 December 2009 / Published online: 16 January 2010
© Springer Science+Business Media B.V. 2009

Abstract Eigenvalue problem for Poincare-Steklov-3 integral equation is reduced to the solution of three transcendental equations for three unknown numbers, moduli of pants. The complete list of antisymmetric eigenfunctions of integral equation in terms of Kleinian membranes is given.

Keywords Spectral parameter · Riemann surface · Pair of pants · Branched complex projective structure · Dessin d’Enfants

Mathematics Subject Classifications (2000) 30Fxx · 14H15 · 30C20 · 45C05 · 33E30

1 Introduction

Traditionally, integral equations are the subject of functional analysis and operator theory. In the contrast we show that methods of complex geometry and combinatorics are efficient for the study of the following singular integral Poincare-Steklov (briefly, PS) equations

$$\lambda \text{V.p.} \int_I \frac{u(t)}{t-x} dt - \text{V.p.} \int_I \frac{u(t) dR(t)}{R(t) - R(x)} = \text{const}, \quad x \in I := (-1, 1), \quad (1)$$

Supported by RFBR grant 09-01-12160 and RAS Program “Contemporary problems of theoretical mathematics”.

A. B. Bogatyrev (✉)
Institute for Numerical Mathematics, Russian Academy of Sciences,
ul. Gubkina 8, 119991 Moscow GSP-1, Russia
e-mail: gourmet@inm.ras.ru

where λ is the spectral parameter; $u(t)$ is the unknown function; $const$ is independent of x . The functional parameter $R(t)$ of the equation is a given smooth *nondegenerate* change of variable on the interval I :

$$0 < \left| \frac{d}{dt} R(t) \right| < \infty, \quad \text{when } t \in [-1, 1]. \quad (2)$$

Under the assumption that $R(t) =: R_3(t)$ is a degree three rational function with separate real critical values different from the endpoints of the interval I , we give the constructive representation for the eigenvalues λ and eigenfunctions $u(x)$ of (1). First, we say a few words about the origin of PS integral equations and the related background.

Spectral Boundary Value Problem Let a domain in the plane be subdivided into two simply connected domains Ω_1 and Ω_2 by a smooth simple arc Γ . We are looking for the values of the spectral parameter λ when the following problem has nonzero solution:

Find a harmonic function U_s in the domain Ω_s , $s = 1, 2$, vanishing on the outer portion of the boundary: $\partial\Omega_s \setminus \Gamma$. On the interface Γ the functions U_1 and U_2 coincide while their normal derivatives differ by the factor of $-\lambda$:

$$-\lambda \frac{\partial U_1}{\partial n} = \frac{\partial U_2}{\partial n}. \quad (3)$$

Applications Boundary value problems for the Laplace equation with spectral parameter in the boundary conditions were first considered by H.Poincare (1896) and V.A.Steklov (1901). The problems of this kind arise e.g. in the analysis of diffraction, (thermo-) conductivity of composite materials and the motion of two-phase liquids in porous medium.

This particular problem (3) arises in justification and optimization of *domain decomposition method* for the solution of boundary values problems for elliptic PDE. The eigenvalues λ of the spectral problem and the traces of eigenfunctions $U_1 = U_2$ on the interface Γ are respectively the critical values and critical points of the following functional, the ratio of two Dirichlet integrals

$$F(U) = \frac{\int_{\Omega_2} |\nabla U_2|^2 d\Omega_2}{\int_{\Omega_1} |\nabla U_1|^2 d\Omega_1}, \quad U \in H_{oo}^{1/2}(\Gamma), \quad (4)$$

where U_s is the harmonic continuation of the function U from interface Γ to the domain Ω_s , $s = 1, 2$, vanishing at the outer boundary of the domain.

Integral Equation The reduction of the stated above boundary value problem to the interface brings to the (1). Let V_s be the harmonic function conjugate to U_s , $s = 1, 2$. From Cauchy-Riemann equations and (3) it follows that tangent to the interface derivatives of V_1 and V_2 differ by the same factor $-\lambda$. Integrating along Γ we get

$$\lambda V_1(y) + V_2(y) = const, \quad y \in \Gamma. \quad (5)$$

For the half-plane the boundary values of conjugate harmonic functions are related via Hilbert transform. To take advantage of this transformation we consider a conformal mapping $\omega_s(y)$ from Ω_s to the open upper halfplane \mathbb{H} with normalization $\omega_s(\Gamma) = I, s = 1, 2$. Now (5) may be rewritten as

$$-\frac{\lambda}{\pi} V.p. \int_I \frac{U_1(\omega_1^{-1}(t))}{t - \omega_1(y)} dt - \frac{1}{\pi} V.p. \int_I \frac{U_2(\omega_2^{-1}(t'))}{t' - \omega_2(y)} dt' = const, \quad y \in \Gamma.$$

Introducing new notation $x := \omega_1(y) \in I; R := \omega_2 \circ \omega_1^{-1} : I \rightarrow \Gamma \rightarrow I; u(t) := U_1(\omega_1^{-1}(t))$ and the change of variable $t' = R(t)$ in the second integral, we arrive at the Poincare-Steklov (1). Note that here $R(t)$ is the decreasing function on I .

Operator analysis of two equivalent spectral problems, boundary value problem (3) and Poincare-Steklov (1), may be found e.g. in [1, 2]. Here we only mention that the spectrum is discreet if (2) holds, the eigen values are positive and converge to $\lambda = 1$.

Philosophy of the Research The aim of our study is to give explicit expressions for the eigen pairs (λ, u) of the PS integral equation. For the rational degree two functions $R(x) = R_2(x)$ the eigen pairs were expressed in terms of elliptic functions [3]. Next natural step is to consider degree three rational functions.

Here the notion of *explicit solution* should be specified. Usually this term means an answer in terms of *elementary function* of parameters or a *quadrature* of it or an application of other *permissible operations* in the spirit of Umemura classical functions. The history of mathematics however knows many disappointing results when the solution of the prescribed form does not exist. The nature always forces us to introduce new types of transcendent objects to enlarge the scope of search. Cf.: “Mais cette étude intime de la nature des fonctions integrales ne peut se faire que par l’introduction de transcendentes nouvelles” [4].

Take for instance the algebraic equations. The ancients were able to solve quadratic equations. But after the invention of the formulas for cubic and quartic equations in the 16th century no progress was made until the 19th century when it became clear that no formula including arithmetic operations and radicals only can solve equations of higher orders. After that Ch.Hermite and L.Kronecker suggested formulae involving elliptic modular function to find the roots of degree five equations. The ideas of C.Jordan elaborated by H.Umemura resulted in a formula (involving hyperelliptic integrals and theta constants) for the roots of arbitrary degree polynomial.

In modern mathematical physics it is very often that the problems are “explicitly” solved in terms of suitable transcendental functions, say solutions of Painleve equations. From the philosophical point of view our goal is to study the nature of the solutions of integral (1) and the means for their constructive representation.

Brief Description of the Result Given rational degree three function $R_3(t)$, we explicitly associate it to a *pair of pants* in Section 2.3. On the other hand, given spectral parameter λ and two auxiliary real parameters, we explicitly construct in Section 4 another pair of pants which additionally depend on one or two integers. When the above two pants are conformally equivalent, λ is the eigenvalue of the PS integral equation with parameter $R_3(x)$. Essentially, this means that to find the spectrum of the given integral (1) one has to solve three transcendental equations involving three *moduli of pants*.

Whether this representation of the solutions may be considered as a constructive or not is a matter of a discussion. Two arguments in favour: today it is possible to numerically evaluate the conformal structure of surfaces (e.g. via circle packing). Also, this representation allows us to conceive the valuable features of the solution: to find the number of zeroes of eigenfunction $u(t)$, to localize the spectrum and to show the discrete mechanism of generating the eigenvalues.

2 Space of PS-3 Equations

In what follows we consider integral equations (1) with *rational degree three real* functional parameter $R(x) = R_3(x)$ and call such equations PS-3. We restrict ourselves to the case when $R_3(x)$ has *four distinct real critical values different from ± 1* . Other possible configurations are discussed in [11]. The details of our further constructions depend on the topological properties of functional parameter of the integral equation. One may encounter one of five described in Section 2.2 typical situations \mathcal{A} , $\mathcal{B}1$, $\mathcal{B}21$, $\mathcal{B}22$, $\mathcal{B}23$ corresponding to the components in the space of admissible functions $R_3(x)$.

2.1 Topology of the Branched Covering

Degree three rational function $R_3(x)$ defines the three-sheeted branched covering of a Riemann sphere by another Riemann sphere. The Riemann-Hurwitz formula suggests that $R_3(x)$ typically has four separate branch points $a_s, s = 1, 4$. This means that every value a_s is covered by a critical point b_s , and an ordinary point c_s . We have assumed that all four points a_s are distinct, real and differ from ± 1 .

Every point $y \neq a_s$ of the extended real axis $\hat{\mathbb{R}} := \mathbb{R} \cup \{\infty\}$ belongs to exactly one of two types. For the type (3:0) the pre-image $R_3^{-1}(y)$ consists of three distinct real points. For the type (1:2) the pre-image consists of a real and two complex conjugate points. The type of the point is locally constant on the extended real axis and changes when we step over the branch point. Let the branch points a_s be enumerated in the natural cyclic order of $\hat{\mathbb{R}}$ so that the intervals (a_1, a_2) and (a_3, a_4) are filled with the points of the type (1:2). We specify the way to exclude the relabeling $a_1 \leftrightarrow a_3, a_2 \leftrightarrow a_4$ of branch points in Section 2.2.

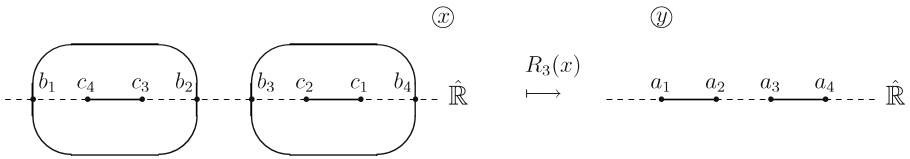


Fig. 1 The topology of the covering R_3 with real branch points

The total pre-image $R_3^{-1}(\hat{\mathbb{R}})$ consists of the extended real axis and two pairs of complex conjugate arcs intersecting $\hat{\mathbb{R}}$ at points b_1, b_2, b_3, b_4 as shown at the left side of Fig. 1. The complement of this pre-image on the Riemann sphere has six components, each of them is mapped 1-1 onto upper or lower half plane. Note that the points $b_1, c_4, c_3, b_2, \dots$ on the left picture of Fig. 1 may follow in inverse order as well.

2.2 Classification of Parameters R_3

The functional parameter $R_3(x)$ is a nondegenerate change of variable on the segment $[-1, 1]$. This in particular means that no critical point b_s belongs to this segment. So exactly one of two cases is realized:¹

$$\begin{aligned} \text{Case } \mathcal{A} : & [-1, 1] \subset [b_2, b_3], \\ \text{Case } \mathcal{B} : & [-1, 1] \subset [b_3, b_4]. \end{aligned} \tag{6}$$

Remaining possibilities (like $[-1, 1] \subset [b_1, b_2]$) are reduced either to \mathcal{A} or \mathcal{B} by the clever choice of labeling the branch points a_s —see Section 2.1. For the case \mathcal{B} it is important whether $[-1, 1]$ intersects $[c_2, c_1]$ or not. So we consider two subcases:

$$\begin{aligned} \text{Case } \mathcal{B1} : & [-1, 1] \cap [c_2, c_1] = \emptyset, \\ \text{Case } \mathcal{B2} : & [-1, 1] \cap [c_2, c_1] \neq \emptyset. \end{aligned} \tag{7}$$

The case $\mathcal{B2}$ in turn is subdivided into three subcases:

$$\begin{aligned} \text{Case } \mathcal{B21} : & [-1, 1] \subset [c_2, c_1], \\ \text{Case } \mathcal{B22} : & [-1, 1] \supset [c_2, c_1], \\ \text{Case } \mathcal{B23} : & \text{all the rest.} \end{aligned} \tag{8}$$

2.3 Pair of Pants Associated to R_3

For the obvious reason, a pair of pants is the name for the Riemann sphere with three holes in it. Pair of pants may be conformally mapped to $\hat{\mathbb{C}}$ with three nonintersecting real slots. This mapping is unique up to real linear-fractional mappings. The conformal class of pants with labelled boundary components depends on three real parameters varying in a cell.

¹Two points on a circle (extended real axis) define two segments. It should be clear which segment we mean: e.g. $b_1, b_2 \notin [b_3, b_4]$; $b_1, b_4 \notin [b_2, b_3]$, etc.

Definition To every PS-3 equation we associate the pair of pants:

$$\mathcal{P}(R_3) := Cl\left(\hat{\mathbb{C}} \setminus \{([-1, 1] \Delta [a_1, a_2]) \cup [a_3, a_4]\}\right) \tag{9}$$

where Δ is the symmetric difference (union of two sets minus their intersection). *Closure* here and everywhere below is taken with respect to the intrinsic spherical metric when every slot acquires two banks. Boundary components of pants are colored in accordance with the palette:

$$\begin{aligned} [-1, 1] \setminus [a_1, a_2] & \text{ - red} \\ [a_1, a_2] \setminus [-1, 1] & \text{ - blue} \\ [a_3, a_4] & \text{ - green} \end{aligned}$$

Thus obtained pair of pants will have boundary ovals of all three colors, but in cases $\mathcal{B}21$ (green and two blue ovals) and $\mathcal{B}22$ (green and two red ovals). Note that in case \mathcal{A} the red, green and blue slots always follow in the natural cyclic order of the extended real axis.

2.4 Gauge Transformations

There is a two-parametric transformation of the functional parameter $R(x)$ which essentially does not affect the spectral characteristics of integral equation (1). Let us recall that $R(x)$ is not uniquely determined by two domains Ω_1 and Ω_2 . Pre- and post- composition with linear-fractional transformations preserving the segment $[-1, 1]$ is admissible. The general appearance of such a mapping is

$$L_\alpha^\pm(t) := \pm \frac{t + \alpha}{\alpha t + 1}, \quad \alpha \in (-1, 1). \tag{10}$$

Lemma 1

1. The gauge transformation $R \rightarrow L_\alpha^\pm \circ R$ does not change neither eigenvalues λ nor the eigenfunctions $u(t)$ of any PS integral equation.
2. The gauge transformation $R \rightarrow R \circ L_\alpha^\pm$ does not change the eigenvalues λ and slightly changes the eigenfunctions: $u(t) \rightarrow u(L_\alpha^\pm(t))$.

Proof To simplify the notations we put $L(t) := L_\alpha^\pm(t)$.

1. The gauge transformation just adds a constant term to the right hand side of equation.

$$\begin{aligned} \int_{-1}^1 \frac{u(t)dL(R(t))}{L(R(t)) - L(R(x))} &= \int_{-1}^1 \frac{u(t)L'(R(t))dR(t)}{[L'(R(t))L'(R(x))]^{1/2}(R(t) - R(x))} \\ &= \int_{-1}^1 \frac{u(t)dR(t)}{R(t) - R(x)} - \int_{-1}^1 \frac{u(t)dR(t)}{R(t) - L^{-1}(\infty)}. \end{aligned}$$

2. We define the new variable $x_* := L(x)$ and the new function $u_*(x_*) := u(x)$.

$$\int_{-1}^1 \frac{u(t)dR(L(t))}{R(L(t)) - R(L(x))} = \pm \int_{-1}^1 \frac{u_*(t_*)dR(t_*)}{R(t_*) - R(x_*)},$$

$$\int_{-1}^1 \frac{u(t)dt}{t - x} = \pm \int_{-1}^1 \frac{u_*(t_*)dL^{-1}(t_*)}{L^{-1}(t_*) - L^{-1}(x_*)} = \pm \int_{-1}^1 \frac{u_*(t_*)dt_*}{t_* - x_*} \mp \int_{-1}^1 \frac{u_*(t)dt}{t - L(\infty)}.$$

We see that essentially the space of $PS - 3$ equations has real dimension 3, the same as the dimension of the moduli space of pants. It is easy to check the following:

- Any gauge transformation of the parameter $R_3(x)$ does not change the type $(\mathcal{A}, \mathcal{B}1, \dots)$ of integral equation.
- The transformation $R_3 \rightarrow R_3 \circ L_\alpha^\pm$ does not change the associated pants (9) and preserves the colors of the boundary ovals.
- Associated to functional parameter $L_\alpha^\pm \circ R_3$ are the pants $L_\alpha^\pm \mathcal{P}(R_3)$. The colors of the boundary ovals are transferred by L_α^\pm , but in one case. When the type of integral equation is \mathcal{A} , the transformation L_α^- interchanges blue and green colours on the boundaries.

2.5 Reconstruction of $R_3(x)$ from the Pants

The parameter $R_3(x)$ of integral equation may be reconstructed, given the pants $\mathcal{P}(R_3)$ and the type $\mathcal{A}, \mathcal{B}1 \dots$ of the equation. One has to follow the routine described below.

Restore the Labeling of the Branch Points In case $\mathcal{B}2$ we temporarily paint the real segment separating two non-green slots in blue. The (extended) blue segment is set to be $[a_1, a_2]$; the green segment is $[a_3, a_4]$. The relabeling $a_1 \leftrightarrow a_2$ and $a_3 \leftrightarrow a_4$ is eliminated by the natural cyclic order of the points a_1, a_2, a_3, a_4 on the extended real axis.

Normalized Covering Let L_a be the unique linear-fractional map sending the points a_1, a_2, a_3, a_4 to respectively $0, 1, a > 1, \infty$. The conformal motion L_b of the covering Riemann sphere sends the critical points b_1, b_2, b_3, b_4 of $R_3(x)$ (unknown at the moment) to respectively $0, 1, b > 1, \infty$. The function $L_a \circ R_3 \circ L_b^{-1}$ with the normalized critical points and critical values takes a simple form:

$$\widetilde{R}_3(x) = x^2 L(x),$$

with real linear fractional function $L(x)$ satisfying the restrictions:

$$\begin{aligned} L(1) &= 1, & L'(1) &= -2, \\ L(b) &= a/b^2, & L'(b) &= -2a/b^3. \end{aligned}$$

We got four equations for three parameters of $L(x)$ and the unknown b . The first two equations suggest the following expression for the linear-fractional function:

$$L(x) = 1 + 2 \frac{(c - 1)(x - 1)}{x - c}.$$

The other two equations are solved parametrically in terms of c :

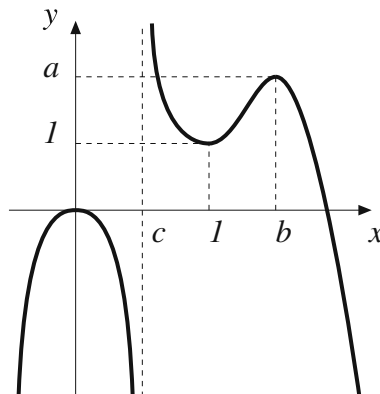
$$b(c) = c \frac{3c - 2}{2c - 1}; \quad a(c) = c \frac{(3c - 2)^3}{2c - 1}.$$

Given $a > 1$, there are exactly two real solutions of the equation $a(c) = a$. One of the solutions c lies in the segment $(1/3, 1/2)$, the other lies in $(1, \infty)$. In the case $c \in (1/3, 1/2)$ the segments $L_a(a_1, a_2) = (0, 1)$ and $L_a(a_3, a_3) = (a, \infty)$ are filled with the points of the type (1:2), which corresponds to our choice of labelling the branchpoints in Section 2.1. The solution $c \in (1, \infty)$ is a fake as the same segments bear the points of the type (3:0). Both functions $b(c)$ and $a(c)$ increase from 1 to ∞ when the argument c runs from $1/3$ to $1/2$.

Reconstruction of the Mapping L_b In case \mathcal{A} the red, green and blue slots follow in the natural cyclic order. Hence, the segment $L_a[-1, 1]$ is a subset of the interval $(1, a)$. We choose the unique component of the pre-image \widetilde{R}_3^{-1} of the segment $L_a[-1, 1]$ belonging to the interval $(1, b)$ – see Fig. 2. For the case \mathcal{B} the segment $L_a[-1, 1]$ is a subset of the ray $(-\infty, a)$ and we choose the pre-image of this segment which lie in (b, ∞) . The requirement: L_b maps $[-1, 1]$ to the chosen segment determines this map up to a pre-composition with the function (10).

We see that given the pants $\mathcal{P}(R_3)$, the functional parameter is recovered up to a gauge transformation $R_3 \rightarrow R_3 \circ L_a^\pm$. It is not difficult to check, that the described above procedure applied to the pair of pants $L_\beta^\pm \mathcal{P}(R_3)$ (in case \mathcal{A} and the mapping L_β^- reversing the orientation of real axis we additionally have

Fig. 2 The graph of $\widetilde{R}_3(x)$ when $c \in (\frac{1}{3}, \frac{1}{2})$



to exchange the blue and green colors of the slots) returns the covering map $L_{\beta}^{\pm} \circ R_3 \circ L_{\alpha}^{\pm}$. Roughly speaking, the classes of gauge transformation of $R_3(x)$ correspond to the conformal classes of pants with suitably colored boundary components and each conformal class of pants corresponds to a class of certain functional parameter $R_3(x)$.

3 Reduction to Projective Structures

PS integral equations possess rich geometrical content [10, 11] which we disclose in this section. We describe a three-step reduction of the integral equation to a certain problem [11] for projective structures on a riemann surface which has essentially combinatorial solution.

3.1 Step 1: Functional Equation

Let us expand the kernel of the second integral in (1) into a sum of elementary fractions:

$$\frac{R'_3(t)}{R_3(t) - R_3(x)} = \frac{d}{dt} \log(R_3(t) - R_3(x)) = \sum_{k=1}^3 \frac{1}{t - z_k(x)} - \frac{Q'}{Q}(t), \tag{11}$$

where $Q(t)$ is the denominator in noncancellable representation of $R_3(t)$ as the ratio of two polynomials; $z_1(x) = x, z_2(x), z_3(x)$ —are all solutions (including multiple and infinite) of the equation $R_3(z) = R_3(x)$. This expansion suggests to rewrite the original equation (1) as certain relationship for the Cauchy-type integral

$$\Phi(x) := \int_I \frac{u(t)}{t - x} dt + const^*, \quad x \in \hat{\mathbb{C}} \setminus [-1, 1]. \tag{12}$$

Known $\Phi(x)$, the solution $u(t)$ may be recovered by the Sokhotskii-Plemelj formula:

$$u(t) = (2\pi i)^{-1} [\Phi(t + i0) - \Phi(t - i0)], \quad t \in I. \tag{13}$$

The constant term $const^*$ in (12), which we assume to be

$$const^* := \frac{1}{\lambda - 3} \left[\int_I \frac{u(t)Q'(t)}{Q(t)} dt - const \right] \tag{14}$$

is introduced to cancel the constant terms arising after substitution of expression (12) to the equation (1). In this way the following result was proven [10]:

Lemma 2 For $\lambda \neq 1, 3$ the transformations (12) and (13) bring about a one-to-one correspondence between the Hölder's eigenfunctions $u(t)$ of PS-3 integral

equation and the holomorphic on the Riemann sphere outside the slot $[-1, 1]$ nontrivial solutions $\Phi(x)$ of the functional equation

$$\Phi(x + i0) + \Phi(x - i0) = \delta \left(\Phi(z_2(x)) + \Phi(z_3(x)) \right), \quad x \in I, \quad (15)$$

$$\delta = 2/(\lambda - 1), \quad (16)$$

with Hölder boundary values $\Phi(x \pm i0)$ at the banks of the slot $[-1, 1]$.

3.2 Step 2: Riemann Monodromy Problem

In this section we reduce our functional (and therefore integral) equation to the Riemann monodromy problem in the following form. *Find a holomorphic vector $W(y) = (W_1, W_2, W_3)^t$ on the slit sphere $\mathcal{P}(R_3) \setminus [-1, 1]$ whose boundary values on the opposite sides of every slot are related by the constant matrix specified for each slot.*

3.2.1 Monodromy Generators

To formulate the Riemann monodromy problem we introduce 3×3 permutation matrices

$$\mathbf{D}_1 := \begin{vmatrix} 1 & 0 & 0 \\ 0 & 0 & 1 \\ 0 & 1 & 0 \end{vmatrix}; \quad \mathbf{D}_2 := \begin{vmatrix} 0 & 0 & 1 \\ 0 & 1 & 0 \\ 1 & 0 & 0 \end{vmatrix}; \quad \mathbf{D}_3 := \begin{vmatrix} 0 & 1 & 0 \\ 1 & 0 & 0 \\ 0 & 0 & 1 \end{vmatrix} \quad (17)$$

and a matrix depending on the spectral parameter λ :

$$\mathbf{D} := \begin{vmatrix} -1 & \delta & \delta \\ 0 & 1 & 0 \\ 0 & 0 & 1 \end{vmatrix}, \quad \delta = 2/(\lambda - 1). \quad (18)$$

Lemma 3 *Matrices $\mathbf{D}_1, \mathbf{D}_2, \mathbf{D}_3, \mathbf{D}, \mathbf{D}_1\mathbf{D} = \mathbf{D}\mathbf{D}_1$ have order two as GL_3 group elements.*

3.2.2 Separating Branches of R_3^{-1}

Let domain \mathcal{O} be the compliment to the segments $[a_1, a_2]$ and $[a_3, a_4]$ on the Riemann sphere. The pre-image $R_3^{-1}\mathcal{O}$ consists of three components $\mathcal{O}_j, j = 1, 2, 3$, mapped one-one to \mathcal{O} —see Fig. 1. Two of the components are (topological) discs with a slot and the third is an annulus. The enumeration of domains \mathcal{O}_j is determined by the following rule: the segment $[-1, 1]$ lies in the closure of \mathcal{O}_1 , the segment $[c_3, c_4]$ lies on the border of \mathcal{O}_2 .

3.2.3

Let $u(x)$ be the solution of integral equation (1) in the case \mathcal{A} . We consider the vector

$$W(y) = (\Phi(x_1), \Phi(x_2), \Phi(x_3))', \quad y \in \mathcal{O} \setminus [-1, 1], \tag{19}$$

where $\Phi(x)$ is from (12) and x_s is the unique solution of the equation $R_3(x_s) = y$ in \mathcal{O}_s . Vector $W(y)$ will be holomorphic and bounded in the domain $\mathcal{O} \setminus [-1, 1]$ as all three points $x_s, s = 1, 2, 3$, remain in the holomorphy domain of the function $\Phi(x)$. We claim that

$$\begin{aligned} W(y + i0) &= \mathbf{D}W(y - i0), & \text{when } y \in [-1, 1], \\ W(y + i0) &= \mathbf{D}_3W(y - i0), & \text{when } y \in [a_1, a_2], \\ W(y + i0) &= \mathbf{D}_2W(y - i0), & \text{when } y \in [a_3, a_4]. \end{aligned}$$

Indeed, let $y^+ := y + i0$ and $y^- := y - i0$ be two points on the opposite banks of $[a_1, a_2]$. Their inverse images $x_3^+ = x_3^-, x_1^\pm = x_2^\mp$ lie outside the cut $[-1, 1]$. Hence $W(y^+) = \mathbf{D}_3W(y^-)$. For two points y^\pm lying on the opposite banks of the slot $[a_3, a_4]$, their inverse images satisfy the relations $x_2^+ = x_2^-, x_1^\pm = x_3^\mp$, which means $W(y^+) = \mathbf{D}_2W(y^-)$. Finally, let y^\pm lie on the banks of $[-1, 1]$. Now two points $x_2^+ = x_2^-$ and $x_3^+ = x_3^-$ lie in the holomorphy domain of $\Phi(x)$ while x_1^+ and x_1^- appear on the opposite sides of the cut $[-1, 1]$. According to the functional equation (15),

$$\Phi(x_1^+) = -\Phi(x_1^-) + \delta(\Phi(x_2^-) + \Phi(x_3^-)),$$

therefore $W(y^+) = \mathbf{D}W(y^-)$ holds on the slot $[-1, 1]$.

3.2.4

Conversely, let $W(y) = (W_1, W_2, W_3)'$ be the bounded solution of the Riemann monodromy problem stated above. We define a piecewise holomorphic function on the Riemann sphere:

$$\Phi(x) := W_s(R_3(x)), \quad \text{when } x \in \mathcal{O}_s \setminus R_3^{-1}[-1, 1], \quad s = 1, 2, 3. \tag{20}$$

From the boundary relations for the vector $W(y)$ it immediately follows that the function $\Phi(x)$ has no jumps on the lifted cuts $[a_1, a_2], [a_3, a_4], [-1, 1]$ apart from the cut $[-1, 1]$ from the upper sphere. Say, if the two points y^\pm lie on the opposite sides of the cut $[a_1, a_2]$, then $W_3(y^+) = W_3(y^-)$ and $W_1(y^\pm) = W_2(y^\mp)$ which means that the function $\Phi(x)$ has no jump on the components of $R_3^{-1}[a_1, a_2]$. From the boundary relation on the cut $[-1, 1]$ it follows that $\Phi(x)$ is the solution for the functional equation (15). Therefore it gives a solution of Poincare- Steklov integral equation with parameter $R_3(x)$. Combining formulae (13) with (20) we get the reconstruction rule

$$u(x) = (2\pi i)^{-1} \left(W_1(R_3(x) + i0) - W_1(R_3(x) - i0) \right), \quad x \in [-1, 1]. \tag{21}$$

3.2.5

We have just proved for the case \mathcal{A} the following

Theorem 1 [11] *If $\lambda \neq 1, 3$ then two formulas (19) and (21) implement the one-to-one correspondence between the solutions $u(x)$ of the integral equation (1) and the bounded solutions $W(y)$ of the Riemann monodromy problem in the slit sphere $\hat{\mathbb{C}} \setminus \{[a_1, a_2] \cup [a_3, a_4] \cup [-1, 1]\}$ with the following matrices assigned to the slots:*

		$[-1, 1] \setminus [a_1, a_2]$		$[a_1, a_2] \setminus [-1, 1]$		$[a_3, a_4]$		$[-1, 1] \cap [a_1, a_2]$		
Case \mathcal{A} :		D		D₃		D₂				
Case $\mathcal{B}1$:		D		D₁		D₂				
Case $\mathcal{B}2$:		D		D₁		D₂		D₁D = DD₁		(22)

3.2.6 Monodromy Invariant

It may be checked that the matrices **D**, **D₁**, **D₂**, **D₃** generating the monodromy group for the solution $W(y)$ are pseudo-orthogonal, that is preserve the same quadratic form

$$J(W) := \sum_{k=1}^3 W_k^2 - \delta \sum_{j<s} W_j W_s. \tag{23}$$

This form is not degenerate unless $-2 \neq \delta \neq 1$, or equivalently $0 \neq \lambda \neq 3$. Since the solution $W(y)$ of our monodromy problem is bounded near the cuts, the value of the form $J(W)$ is independent of the variable y . Therefore the solution ranges either in the smooth quadric $\{W \in \mathbb{C}^3 : J(W) = J_0 \neq 0\}$, or the cone $\{W \in \mathbb{C}^3 : J(W) = 0\}$.

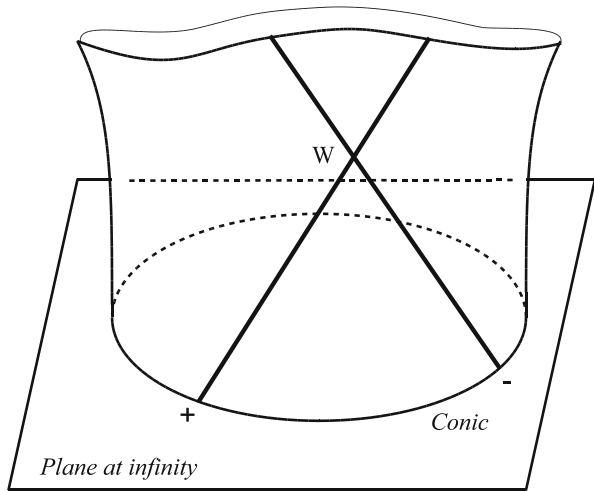
3.2.7 Geometry of Quadric Surface

The nondegenerate projective quadric $\{J(W) = J_0\}$ contains two families of line elements which for convenience we denote by the signs '+' and '-'. Two different lines from the same family are disjoint while two lines from different families intersect. The intersection of those lines with the 'infinitely distant' secant plane gives points on the conic

$$\{(W_1 : W_2 : W_3)^t \in \mathbb{CP}^2 : J(W) = 0\} \tag{24}$$

which by means of stereographic projection p may be identified with the Riemann sphere. Therefore we have introduced two global coordinates $p^\pm(W)$ on the quadric, 'infinite part' of which (i.e. conic (24)) corresponds to coinciding coordinates: $p^+ = p^-$ (see Fig. 3).

Fig. 3 Global coordinates p^+ and p^- on quadric



To obtain explicit expressions for the coordinate change $W \leftrightarrow p^\pm$ on quadric we bring the quadratic form $J(W)$ to the simpler form $J_\bullet(V) := V_1 V_3 - V_2^2$ by means of the linear coordinate change

$$W = \mathbf{K}V \tag{25}$$

where

$$\mathbf{K} := (3\delta + 6)^{-1/2} \begin{pmatrix} 1 & 1 & 1 \\ 1 & \varepsilon^2 & \varepsilon \\ 1 & \varepsilon & \varepsilon^2 \end{pmatrix} \cdot \begin{pmatrix} 0 & \mu^{-1} & 0 \\ 0 & 0 & 1 \\ 1 & 0 & 0 \end{pmatrix}, \tag{26}$$

$$\varepsilon := \exp(2\pi i/3), \quad \mu := \sqrt{\frac{\delta - 1}{\delta + 2}} = \sqrt{\frac{3 - \lambda}{2\lambda}}.$$

Translating the first paragraph of the current section into the language of formulae we get

$$p^\pm(W) := \frac{V_2 \pm i\sqrt{J_0}}{V_1} = \frac{V_3}{V_2 \mp i\sqrt{J_0}}; \tag{27}$$

and inverting this dependence,

$$W(p^+, p^-) = \frac{2i\sqrt{J_0}}{p^+ - p^-} \mathbf{K} \begin{pmatrix} 1 \\ (p^+ + p^-)/2 \\ p^+ p^- \end{pmatrix}. \tag{28}$$

The point $W(p^+, p^-)$ with coordinate p^+ (resp. p^-) being fixed moves along the straight line with the directing vector $\mathbf{K}(1 : p^+ : (p^+)^2)$ (resp. $\mathbf{K}(1 : p^- : (p^-)^2)$) belonging to the conic (24).

Lemma 4 *There exists a (spinor) representation $\chi : O_3(J) \rightarrow PSL_2(\mathbb{C})$ such that:*

- 1) *The restriction of $\chi(\cdot)$ to $SO_3(J)$ is an isomorphism to $PSL_2(\mathbb{C})$.*
- 2) *For coordinates p^\pm on the quadric the following transformation rule holds:*

$$\begin{aligned} p^\pm(\mathbf{T}W) &= \chi(\mathbf{T})p^\pm(W), & \mathbf{T} &\in SO_3(J), \\ p^\pm(\mathbf{T}W) &= \chi(\mathbf{T})p^\mp(W), & \mathbf{T} &\in O_3(J) \setminus SO_3(J). \end{aligned} \tag{29}$$

- 3) *The linear-fractional mapping $\chi p := (ap + b)/(cp + d)$ is the image of the matrix:*

$$\mathbf{T} := \frac{1}{ad - bc} \mathbf{K} \begin{vmatrix} d^2 & 2cd & c^2 \\ bd & ad + bc & ac \\ b^2 & 2ab & a^2 \end{vmatrix} \mathbf{K}^{-1} \in SO_3(J). \tag{30}$$

- 4) *The generators of the monodromy group are mapped to the following elements:*

$$\begin{aligned} \chi(\mathbf{D}_s)p &= \varepsilon^{1-s}/p, & s &= 1, 2, 3; \\ \chi(\mathbf{D})p &= \frac{\mu p - 1}{p - \mu}. \end{aligned} \tag{31}$$

Proof We define the action of matrix $\mathbf{A} \in SL_2(\mathbb{C})$ on the vector $V \in \mathbb{C}^3$ by the formula:

$$\mathbf{A} := \begin{vmatrix} a & b \\ c & d \end{vmatrix} : \begin{vmatrix} V_3 & V_2 \\ V_2 & V_1 \end{vmatrix} \longrightarrow \mathbf{A} \begin{vmatrix} V_3 & V_2 \\ V_2 & V_1 \end{vmatrix} \mathbf{A}^t. \tag{32}$$

It is easy to check that (32) gives the faithful representation of connected 3-dimensional group $PSL_2(\mathbb{C}) := SL_2(\mathbb{C})/\{\pm \mathbf{1}\}$ into $SO_3(J_\bullet)$ and therefore, an isomorphism. Let us denote χ_\bullet the inverse isomorphism $SO_3(J_\bullet) \rightarrow PSL_2(\mathbb{C})$ and let $\chi(\pm \mathbf{T}) := \chi_\bullet(\mathbf{K}^{-1}\mathbf{T}\mathbf{K})$ for $\mathbf{T} \in SO_3(J)$. The obtained homomorphism $\chi : O_3(J) \rightarrow PSL_2(\mathbb{C})$ will satisfy statement 1) of the lemma.

To prove 2) we replace vector V components in the right-hand side of (32) with their representation in terms of the stereographic coordinates p^\pm :

$$\begin{aligned} & \frac{i\sqrt{J_0}}{p^+ - p^-} \mathbf{A} [(p^+, 1)^t \cdot (p^-, 1) + (p^-, 1)^t \cdot (p^+, 1)] \mathbf{A}^t \\ &= i\sqrt{J_0} \frac{(cp^+ + d)(cp^- + d)}{p^+ - p^-} [(\chi p^+, 1)^t \cdot (\chi p^-, 1) + (\chi p^-, 1)^t \cdot (\chi p^+, 1)] \\ &= \frac{i\sqrt{J_0}}{\chi p^+ - \chi p^-} [(\chi p^+, 1)^t \cdot (\chi p^-, 1) + (\chi p^-, 1)^t \cdot (\chi p^+, 1)] \\ &= \left\| \begin{vmatrix} V_3(\chi p^+, \chi p^-) & V_2(\chi p^+, \chi p^-) \\ V_2(\chi p^+, \chi p^-) & V_1(\chi p^+, \chi p^-) \end{vmatrix} \right\|, \end{aligned}$$

where we set $\chi p := (ap + b)/(cp + d)$. Now (29) follows immediately for $\mathbf{T} \in SO_3(J)$. It remains to check the transformation rule for any matrix \mathbf{T} from the other component of the group $O_3(J)$, say $\mathbf{T} = -\mathbf{1}$.

Writing the action (32) component-wise we arrive at conclusion 3) of the lemma.

An finally, expressions 4) for the generators of monodromy group may be obtained either from analyzing formula (30) or finding the eigenvectors of the matrices \mathbf{D}_s, \mathbf{D} which correspond to the fixed points of linear- fractional transformations. □

3.3 Step 3: Projective Structures

Speaking informally, a (branched) complex projective structure [5–9] on the Riemann surface M is a meromorphic function p on the universal cover \tilde{M} of the surface that transforms linear fractionally under the deck transformations. The appropriate representation $\pi_1(M) \rightarrow PSL_2(\mathbb{C})$ is called the *monodromy* of the structure p . The projective structure is called branched when p has critical points. The set of all critical points of $p(t)$ with their multiplicities survives under the cover transformations of \tilde{M} . The projection of this set to the Riemann surface M is known as the *branching divisor* $D(p)$ of projective structure and the branching number of the structure $p(t)$ is $\text{deg } D(p)$. The classical examples of unbranched projective structures arise in Fuchsian or Schottky uniformization of Riemann surfaces.

3.3.1 Projective Structures Generated by Eigenfunction

Stereographic coordinates $p^\pm(y) := p^\pm(W(y))$ for the solution of the Riemann monodromy problem (22) will give two nowhere coinciding meromorphic functions in the sphere with three possibly overlapping slots. As it follows from the transformation rules (29), the boundary values of two functions $p^\pm(y)$ on the slot D_* , one of $[a_1, a_2] \setminus [-1, 1], [-1, 1] \setminus [a_1, a_2], [a_1, a_2] \cap [-1, 1]$ or $[a_3, a_4]$, are related by the formulas

$$\begin{aligned} p^\pm(y + i0) &= \chi(\mathbf{D}_*)p^\mp(y - i0), & y \in D_* \neq [a_1, a_2] \cap [-1, 1], \\ p^\pm(y + i0) &= \chi(\mathbf{DD}_1)p^\pm(y - i0), & y \in [a_1, a_2] \cap [-1, 1], \end{aligned} \tag{33}$$

where \mathbf{D}_* is the matrix assigned to the slot D_* in (22).

Relations (33) allow us to analytically continue both functions $p^+(y)$ and $p^-(y)$ through any slot to locally single valued functions on the genus 2 Riemann surface

$$M := \left\{ w^2 = (y^2 - 1) \prod_{s=1}^4 (y - a_s) \right\}, \tag{34}$$

since all matrices \mathbf{D}_* are involutive—see Lemma 3. Further continuation gives single valued functions $p^\pm(\cdot)$ on the universal covering \tilde{M} . Traveling of the argument y along the handle of the surface M may result in the

linear- fractional transformation of the value $p^\pm(y)$. Say, the continuations of $p^+(y)$ from the pants through the red and green slots will give two different functions on the second sheet related by the linear-fractional mapping $\chi(\mathbf{DD}_2)$.

3.3.2 Branching of Structures p^\pm

The way we have carried out the continuation of functions $p^\pm(y)$ suggests that the branching divisors of the arising projective structures are related via formula:

$$D(p^+) = HD(p^-) \tag{35}$$

where $H(y, w) := (y, -w)$ is the hyperelliptic involution of the surface M . We determine the branching numbers of the structures in the proof of

Theorem 2 [11] *When $\lambda \notin \{0, 1, 3\}$ the solutions $u(x)$ of the PS-3 integral equation are in one-one correspondence with the couples of meromorphic in the slit sphere $\hat{\mathbb{C}} \setminus \{[a_1, a_2] \cup [a_3, a_4] \cup [-1, 1]\}$ functions $p^\pm(y)$ with boundary values satisfying (33) and either non or two critical points in common. The correspondence $u(x) \rightarrow p^\pm(y)$ is implemented by the sequence of formulae (12), (19) and (27). The inverse dependence is given up to proportionality by the formula*

$$u(x) = \sqrt{\frac{\Omega(y)}{dp^+(y)dp^-(y)}}(p^+(y)p^-(y) - \mu(p^+(y) + p^-(y)) + 1), \tag{36}$$

where $x \in [-1, 1]$ and $y := R_3(x) + i0$, $\Omega(y) = (y - y_1)(y - y_2)\frac{(dy)^2}{w^2(y)}$ is the holomorphic quadratic differential on the Riemann surface M with zeroes at the critical points of the (possibly coinciding) functions p^+ and p^- , or with double zeroes $y_1 = y_2$ (otherwise arbitrary) when $p^+ = p^-$ is unbranched.

Remark The number of the critical points of the structures in the slit sphere is counted with their *weight and multiplicity*: 1) the branching number of $p^\pm(y)$ at the branch point $a \in \{\pm 1, a_1, \dots, a_4\}$ of the surface M is computed with respect to the local parameter $z = \sqrt{y - a}$, 2) every critical point on the boundary should be considered as a half-point.

Proof

1. Let $u(x)$ be an eigenfunction of integral equation PS-3. The stereographic coordinates $p^\pm(y)$ of the solution $W(y)$ of the associated Riemann monodromy problem are nowhere equal meromorphic functions when the invariant $J_0 \neq 0$, or two identically equal functions when $J_0 = 0$. In any case they inherit the boundary relationship (33).

What remains is to find the branching numbers of the entangled structures $p^\pm(y)$. To this end we consider the $O_3(J)$ -invariant quadratic differential form $J(dW) = J_\bullet(dV)$ transferred to the slit sphere.

In the general case $J_0 \neq 0$ we get (up to proportionality) the Kleinian quadratic differential:

$$\Omega(y) = \frac{dp^+(y)dp^-(y)}{(p^+(y) - p^-(y))^2}, \quad y \in \hat{\mathbb{C}}. \tag{37}$$

This expression is the infinitesimal form of the cross ratio, hence it remains unchanged after the same linear-fractional transformations of the functions p^+ and p^- . Therefore, (37) is a well defined quadratic differential on the entire sphere. Lifting $\Omega(y)$ to the surface M we get a holomorphic differential. Indeed, $p^+ \neq p^-$ everywhere and applying suitable linear-fractional transformation we assume that $p^+ = 1 + z^{m_+} + \{\text{terms of higher order}\}$ and $p^- = cz^{m_-} + \dots$ in terms of local parameter z of the surface, $m_\pm \geq 1, c \neq 0$. Then $\Omega = cm_+m_-z^{m_++m_- - 2}(dz)^2 + \{\text{terms of higher order}\}$. Therefore

$$D(p^+) + D(p^-) = (\Omega).$$

Any holomorphic quadratic differential on genus 2 surface has 4 zeroes. The curve M consists of two copies of the slit sphere interchanged by the hyperelliptic involution H . Taking into account the symmetry (35) of branching divisors, we see that the structures p^\pm together have two critical points in the slit sphere.

In the special case $J_0 = 0$ two structures merge: $p^\pm(y) =: p(y)$ and the same quadratic differential $J(dW) = J_\bullet(dV)$ on the curve M has the appearance:

$$\Omega(y) = [V_1(y)dp(y)]^2, \tag{38}$$

here $V_1(y)$ is the first component in the vector $V(y)$ defined by formula (25). The analysis of this representation in local coordinates suggests that

$$2D(p) + 2(W) = (\Omega), \tag{39}$$

where (W) is the divisor of zeroes of the locally holomorphic (but globally multivalued) on M vector $W(y)$. To characterize (W) we need the following lemma, which we prove at the end of the current section.

Lemma 5 *The vector $W(y)$ cannot have simple zeroes at the fixed points of the hyperelliptic involution of M when $J_0 = 0$ and $\lambda \neq 0, 3$.*

The divisor (W) is obviously invariant under the hyperelliptic involution H . From this Lemma it follows that either $(W) = 0$ (therefore $\text{deg } D(p) = 2$) or (W) consists of two points interchanged by H (therefore the structure p is unbranched). In other words, $p(y)$ has the branching number 0 or 1 on the slit sphere and the quadratic differential Ω is a square of a holomorphic linear differential.

2. Conversely, let $p^+(y)$ and $p^-(y)$ be two not identically equal meromorphic functions on the slit sphere, with boundary conditions (33) and the

total branching number either zero or two (see remark above). For the meromorphic quadratic differential (37) on the Riemann surface M we establish (using local coordinate on the surface) the inequality:

$$D(p^+) + D(p^-) \geq (\Omega) \tag{40}$$

where the deviation from equality means that there is a point where $p^+ = p^-$. But the degree of the divisor on the left of (40) is zero or four and $\text{deg}(\Omega) = 4$. Therefore, $p^+ \neq p^-$ everywhere (and the total branching of this pair of functions in the slit sphere is two).

The holomorphic vector $W(p^+(y), p^-(y))$ in the slit sphere solves the Riemann monodromy problem specified in Theorem 1. We already know how to convert the latter vector to the eigenfunction of integral equation PS-3. Careful computation gives the restoration formula

$$2\pi u(x) = \sqrt{\frac{(\delta + 2)J_0}{3} \frac{p^+(y)p^-(y) - \mu(p^+(y) + p^-(y)) + 1}{p^+(y) - p^-(y)}}, \tag{41}$$

where $x \in [-1, 1]$ and $y := R_3(x) + i0$. Formula (36) appears after the substitution of (37) to the latter formula.

Finally, suppose that two functions $p^\pm(y)$ with necessary branching and boundary behaviour are identical. For the solution on the cone, $V = V_1 (1, p, p^2)^t$ and the first component V_1 may be taken from (38). Therefore we consider the vector on the slit sphere:

$$W(y) := \frac{(y - y_1)}{w(y)p'(y)} \mathbf{K}(1, p(y), p^2(y))^t, \tag{42}$$

where y_1 is the critical point of $p(y)$ or arbitrary point when $p(y)$ is unbranched. One immediately checks that it is holomorphic and solves the Riemann monodromy problem specified in Theorem 1. Now to find the corresponding eigenfunction is a routine task. □

Proof of Lemma 5 Let the hyperelliptic involution H changes the sign of the local coordinate z defined in the vicinity of the fixed point $z = 0$ of the involution. Boundary relationship of the vector W on the slots implies the symmetry:

$$W(-z) = \mathbf{D}_* W(z) \tag{43}$$

where \mathbf{D}_* is one of the matrices $\mathbf{D}_1, \mathbf{D}_2, \mathbf{D}_3$ or \mathbf{D} . Suppose that W has a simple zero at the fixed point: $W(z) = W^- z + \{\text{terms of higher order}\}$. We immediately see that $W^- \neq 0$ is the eigenvector of \mathbf{D}_* corresponding to eigenvalue -1 of this matrix. Another obvious property of this vector: $J(W^-) = 0$.

The matrix \mathbf{D}_* has the invariant (complex) plane corresponding to the double eigenvalue $+1$. The nullset of the quadratic form $J(\cdot)$ on this plane is nontrivial, in other words there is an eigenvector $W^+ = \mathbf{D}_* W^+ \neq 0$ lying in the cone: $J(W^+) = 0$. The chain of equalities is valid:

$$J(W^+, W^-) = J(\mathbf{D}_* W^+, \mathbf{D}_* W^-) = -J(W^+, W^-) = 0,$$

where $J(\cdot, \cdot)$ is the bilinear form polar to the quadratic form $J(\cdot)$. Now we see that the cone contains the entire plane generated by the vectors W^+ and W^- . Therefore, the quadratic form $J(\cdot)$ is degenerate which only happens when $\lambda = 0, 3$. □

3.4 Mirror Symmetry of Solution

In what follows we are looking for *real* solutions $u(x)$ of the integral equation (1). There is no loss of the generality. Indeed, the restrictions on the monodromy of projective structures [11] imply that the spectrum of any PS-3 integral equation belongs to the segment $[0, 3]$. Now both real and imaginary parts of any complex eigenfunction $u(x)$ are the solutions of the integral equation.

Real solutions $u(x)$ of the integral equation correspond to the solutions of Riemann monodromy problem with mirror symmetry: $W(\bar{y}) = \overline{W(y)}$. This symmetry for the vector $V(y) := \mathbf{K}^{-1}W(y)$ takes the form $V(\bar{y}) = (\overline{V_3(y)} \operatorname{sign}(\delta + 2), \overline{V_2(y)} \operatorname{sign}(\delta - 1), \overline{V_1(y)} \operatorname{sign}(\delta + 2))$. The values $\delta + 2$ and $\delta - 1$ have the same sign as it follows from the range of spectral parameter $\lambda \in [0, 3]$. Therefore, real solutions are split into two classes depending on the sign of $(\delta + 2)J_0$:

$$\begin{aligned} \text{Symmetric } ((\delta+2)J_0 > 0), & \quad p^\pm(\bar{y}) = 1/\overline{p^\pm(y)} \\ \text{Antisymmetric } ((\delta+2)J_0 \leq 0), & \quad p^\pm(\bar{y}) = 1/p^\mp(y), \end{aligned} \quad y \in \mathcal{P}(R_3) \setminus [-1, 1],$$

In the remaining part of the article we give explicit parametrization of all antisymmetric solutions for the integral PS-3 equations of the considered type—when six points $\pm 1, a_1, \dots, a_4$ are real and pairwise distinct.

Restricting ourselves to the search of antisymmetric solutions we have to find only one function in the pants, say $p(y) := p^+(y)$ while the remaining function may be recovered from the mirror antisymmetry:

$$p^-(y) = 1/\overline{p^+(\bar{y})}. \tag{44}$$

On the boundary components of the slit sphere this function obeys the rule:

$$\begin{aligned} p^+(y \pm i0) &\stackrel{(33)}{=} \chi(\mathbf{D}_*)p^-(y \mp i0) \stackrel{(44)}{=} \chi(\mathbf{D}_*\mathbf{D}_1)\overline{p^+(y \pm i0)}, \\ &y \in D_* \neq [-1, 1] \cap [a_1, a_2]. \end{aligned}$$

Therefore

$$\begin{aligned} p &\in \hat{\mathbb{R}}, && \text{when } \mathbf{D}_* = \mathbf{D}_1; \\ p &\in \varepsilon\hat{\mathbb{R}}, && \text{when } \mathbf{D}_* = \mathbf{D}_2; \\ p &\in \varepsilon^2\hat{\mathbb{R}}, && \text{when } \mathbf{D}_* = \mathbf{D}_3; \end{aligned}$$

and finally when $\mathbf{D}_* = \mathbf{D}$, the value of p lies on the circle

$$C := \{ p \in \mathbb{C} : |p - \mu^{-1}|^2 = \mu^{-2} - 1 \}, \quad \mu := \sqrt{\frac{3 - \lambda}{2\lambda}} \tag{45}$$

As an immediate consequence of this observation we give a universal restriction for the spectrum of our integral equation.

Lemma 6 *Antisymmetric eigenfunctions correspond to eigenvalues $\lambda \in [1, 3]$.*

Proof For the cases $\mathcal{A}, \mathcal{B}1, \mathcal{B}22, \mathcal{B}23$ the slot $[-1, 1] \setminus [a_1, a_2]$ is not empty and the boundary value of $p(y)$ on this slot belongs to the circle C . This circle is an empty set for $\mu > 1$, or equivalently $\lambda \in (0, 1)$. The proof for the remaining case $\mathcal{B}21$ requires special machinery and will be given in Section 7. \square

The critical points of two functions $p^+(y)$ and $p^-(y)$ in the considered antisymmetric case are complex conjugate as it follows from (44). Taking this fact into account we reformulate Theorem 2 for the antisymmetric solutions:

Theorem 3 *When $\lambda \notin \{0, 1, 3\}$, the antisymmetric solutions $u(x)$ of integral equation PS-3 are in one-two correspondence with the meromorphic in the slit sphere $\hat{\mathbb{C}} \setminus \{[a_1, a_2] \cup [a_3, a_4] \cup [-1, 1]\}$ functions $p(y)$ that have either none or one critical point in the domain and the following values on the boundary components:*

$y \in$	$[-1, 1] \setminus [a_1, a_2]$ (red)	$[a_1, a_2] \setminus [-1, 1]$ (blue)	$[a_3, a_4]$ (green)
$p(y \pm i0) \in$	C	$\varepsilon^2 \hat{\mathbb{R}}$ (Case \mathcal{A}) $\hat{\mathbb{R}}$ (Case \mathcal{B})	$\varepsilon \hat{\mathbb{R}}$

In case $\mathcal{B}2$ the function $p(y)$ has the jump on the remaining part of the boundary:

$$p(y + i0) = \chi(\mathbf{DD}_1)p(y - i0), \quad y \in [-1, 1] \cap [a_1, a_2]. \tag{46}$$

Remark By 'one-two' correspondence we mean the following: given any function $p(y)$ satisfying the conditions of this theorem, it's easy to check that its antisymmetrization $1/\overline{p(\bar{y})}$ also satisfies all the conditions. Therefore, we have a correspondence of an eigenfunction $u(x)$ to a couple: function $p(y)$ and its antisymmetrization, only one of them being independent.

4 Statement of the Main Result

From the Section 3.4 it follows that every antisymmetric eigenfunction $u(x)$ of PS-3 integral equation induces a mapping $p(y)$ of the pants $\mathcal{P}(R_3)$ to a multivalent domain spread possibly with branching over the Riemann sphere. Such surface is known as Kleinian membrane or Überlagerungsfläche and the complete list of them is given in this section.

4.1 Tailoring the Pants

We define pants $\mathcal{PQ}(\lambda, h_1, h_2 | m_1, \dots)$ of several fashions \mathcal{Q} which parametrically depend on spectral parameter λ , two other reals h_1, h_2 and one or two integers m_1, \dots . Each boundary oval of our pair of pants covers a circle and acquires its color in the following way:

$$\begin{aligned} C & \quad \text{-- red,} \\ \varepsilon \hat{\mathbb{R}} \text{ or } \chi(\mathbf{DD}_1) \varepsilon \hat{\mathbb{R}} & \quad \text{-- green,} \\ \hat{\mathbb{R}} \text{ or } \varepsilon^2 \hat{\mathbb{R}} & \quad \text{-- blue.} \end{aligned}$$

Any constructed pair of pants may be obtained from the ‘‘basic’’ pants $\mathcal{PQ}(\lambda, h_1, h_2 | \dots)$ with lowest possible integer parameters by a surgery procedure known as ‘‘grafting’’ and introduced independently by B.Maskit, D.Hejhal and D.Sullivan–W.Thurston in 1969-1983.

4.1.1 Cases $\mathcal{A}, B1$

For real $\lambda \in (1, 2)$ we consider (depending on λ) open annulus α bounded by two circles: C defined in (45) and $\varepsilon \hat{\mathbb{R}}$. Another annulus bounded by C and $\varepsilon^2 \hat{\mathbb{R}}$ we denote $\bar{\alpha}$. Note that for the considered values of λ the circle C does not intersect the lines $\varepsilon^{\pm 1} \hat{\mathbb{R}}$. The m -sheeted unbranched covering of the annuli, $m = 1, 2, \dots$, we denote as $m \cdot \alpha$ or $m \cdot \bar{\alpha}$ correspondingly.

The annuli we have just introduced may be sewn together in the way specified in Table 1 to get the pants of four fashions $\mathcal{PA}_1, \mathcal{PA}_2, \mathcal{PA}_3, \mathcal{PB}1$.

Sign ‘+’ in the definitions of Table 1 means certain surgery explained below.

Instructions on sewing annular patches together

1. $\mathcal{PA}_1(\lambda, h_1, h_2 | m_1, m_2)$. Take two annuli $m_1 \cdot \alpha$ and $m_2 \cdot \bar{\alpha}$. Cut the top sheet of each annulus along the same segment (dashed red line in the Fig. 4) starting at the point $h := h_1 + ih_2$ and ending at the circle C . Now sew the left bank of one cut on the right bank of the other. The emerging surface is the pair of pants.

Table 1 Three-parametric families of pairs of pants for the cases $\mathcal{A}, B1$; parameter $1 < \lambda < 2$

Fashion of pants	Range of h_1, h_2 and m_1, m_2	Definition
$\mathcal{PA}_1(\lambda, h_1, h_2 m_1, m_2)$	$h := h_1 + ih_2 \in \alpha \cap \bar{\alpha}, h \geq 1;$ $m_1, m_2 = 1, 2, \dots$	$Cl\{(m_1 \cdot \alpha) \setminus [\mu^{-1}, h]\} +$ $Cl\{(m_2 \cdot \bar{\alpha}) \setminus [\mu^{-1}, h]\}$
$\mathcal{PA}_2(\lambda, h_1, h_2 m_1, m_2)$	$0 < h_1 < h_2, h_1 h_2 \geq 1;$ $m_1 = 1, 2, \dots, m_2 = 0, 1, 2, \dots$	$Cl\{(m_1 \cdot \alpha) \setminus \{-\varepsilon^2[h_1, h_2]\}\} +$ $Cl\{m_2 \cdot \bar{\alpha}\}$
$\mathcal{PA}_3(\lambda, h_1, h_2 m_1, m_2)$	$0 < h_1 < h_2, h_1 h_2 \geq 1;$ $m_1 = 0, 1, 2, \dots, m_2 = 1, 2, 3, \dots$	$Cl\{(m_2 \cdot \bar{\alpha}) \setminus \{-\varepsilon[h_1, h_2]\}\} +$ $Cl\{m_1 \cdot \alpha\}$
$\mathcal{PB}1(\lambda, h_1, h_2 m)$	$\mu^{-1} + \sqrt{\mu^{-2} - 1} < h_1 < h_2;$ $m = 1, 2, 3, \dots$	$Cl\{(m \cdot \alpha) \setminus [h_1, h_2]\}$

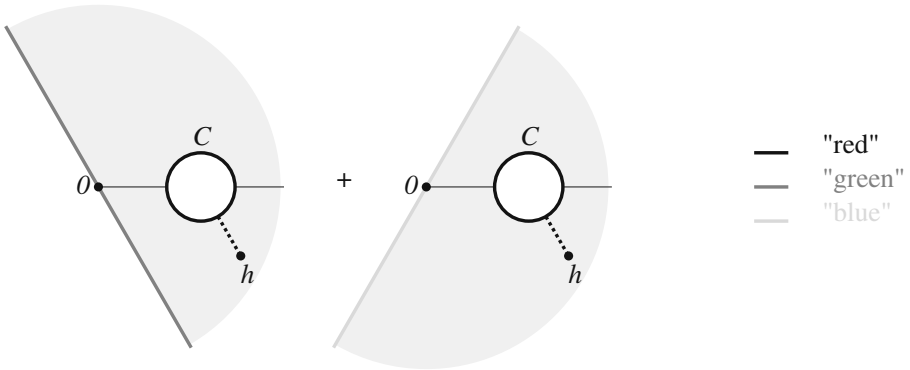


Fig. 4 The pair of pants $\mathcal{P}A_1(\lambda, h_1, h_2 | m_1, m_2)$ is sewn down of two annuli

2. $\mathcal{P}A_2(\lambda, h_1, h_2 | m_1, m_2)$. The annulus $m_1 \cdot \alpha$ with the segment $-\varepsilon^2[h_1, h_2]$ removed from the top sheet is a pair of pants $\mathcal{P}A_2(\lambda, h_1, h_2 | m_1, 0)$. Cut the obtained pair of pants along the segment joining the circle C to the slot (dashed blue line in the Fig. 5). Also cut top sheet of the annulus $m_2 \cdot \bar{\alpha}$ along the same segment and sew the left bank of one cut on the right bank of the other. The arising surface is the pair of pants.
3. $\mathcal{P}A_3(\lambda, h_1, h_2 | m_1, m_2)$. The annulus $m_2 \cdot \bar{\alpha}$ with the segment $-\varepsilon[h_1, h_2]$ removed from the top sheet, is a pair of pants $\mathcal{P}A_3(\lambda, h_1, h_2 | 0, m_2)$. As in the previous passage, we may sew in the annulus $m_1 \cdot \alpha$ to the obtained pants to get the result.
4. $\mathcal{P}B_1(\lambda, h_1, h_2 | m)$ is just the annulus $m \cdot \alpha$ with the segment $[h_1, h_2]$ removed from its top sheet.

The limit case of the pants $\mathcal{P}A_1$, when the branch point $h_1 + ih_2$ tends to $\varepsilon^{\pm 1}\mathbb{R}$, coincides with the limit cases of pants $\mathcal{P}A_2$ or $\mathcal{P}A_3$, when $h_1 = h_2 > 0$. The corresponding unstable two-parametric families of pants $\mathcal{P}A_{12}$ and $\mathcal{P}A_{13}$ are defined in Table 2.

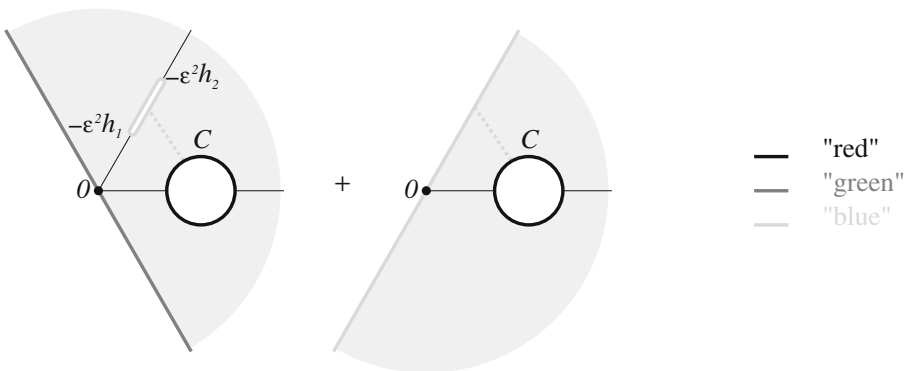


Fig. 5 The pair of pants $\mathcal{P}A_2(\lambda, h_1, h_2 | m_1, m_2)$ is sewn of simpler pants and the annulus

Table 2 Unstable two-parametric families of pants

Fashion of pants	Definition
$\mathcal{PA}_{12}(\lambda, h m_1, m_2)$	$\mathcal{PA}_1(\lambda, -Re(\varepsilon^2 h), -Im(\varepsilon^2 h) m_1, m_2) =$ $\mathcal{PA}_2(\lambda, h, h m_1, m_2)$
$\mathcal{PA}_{13}(\lambda, h m_1, m_2)$	$\mathcal{PA}_1(\lambda, -Re(\varepsilon h), -Im(\varepsilon h) m_1, m_2) =$ $\mathcal{PA}_3(\lambda, h, h m_1, m_2)$

The range of parameters: $1 < \lambda < 2, h > 0, m_1$ and $m_2 = 1, 2, 3, \dots$

4.1.2 Case $\mathcal{B}2$

Two circles: $\varepsilon \hat{\mathbb{R}}$ and $\chi(\mathbf{DD}_1) \varepsilon \hat{\mathbb{R}}$ do not intersect when $\lambda \in (1, 3)$. They bound the open annulus β depending on λ . The m -sheeted unbranched covering of the annulus we denote as $m \cdot \beta, m = 1, 2, 3, \dots$. The points of the annulus $m \cdot \beta$ may be described in the form

$$p = \mu^{-1} + \rho \exp(i\phi),$$

where $\rho > 0$ and the argument $\phi \in \mathbb{R} \text{ mod } 2\pi m$. The action of $\chi(\mathbf{DD}_1)$ on the sphere (i.e. consecutive reflections in circles C and $\hat{\mathbb{R}}$) lifts to the involution of the multi-sheeted annulus $m \cdot \beta$ in the following way:

$$\Xi : \mu^{-1} + \rho \exp(i\phi) \rightarrow \mu^{-1} + \frac{r^2}{\rho} \exp(-i\phi) \tag{47}$$

where $r := \sqrt{\mu^{-2} - 1}$ is the radius of the circle C .

Definition We introduce three pairs of pants $\mathcal{PB}21, \mathcal{PB}22$ and $\mathcal{PB}23$, each of them depend on three reals λ, h_1, h_2 and an integer m :

$$\mathcal{PB}2s(\lambda, h_1, h_2 | m) := Cl\{(m \cdot \beta) \setminus (E_s^1(h_1) \cup E_s^2(h_2))\} / \Xi, \quad s = 1, 2, 3,$$

Table 3 Slots for the subcases of $\mathcal{B}2$, parameter $1 < \lambda < 3$

Definition of slots	Range of h_1, h_2
$E_1^1(h_1) := \mu^{-1} + r \exp[-h_1, h_1],$ $E_1^2(h_2) := \mu^{-1} + r \exp[-h_2, h_2] \exp(i\pi m)$	$h_1 \geq h_2 > 0,$ when m is even; $(\mu^{-1} + r \exp h_1) \cdot$ $(\mu^{-1} - r \exp h_2) \geq 1,$ when m is odd.
$E_2^1(h_1) := \mu^{-1} + r \exp[-ih_1, ih_1],$ $E_2^2(h_2) := \mu^{-1} + r \exp[-ih_2, ih_2] \exp(i\pi m)$	$h_1 \geq h_2,$ when m is even; $\text{Arg}(\exp(ih_1) + \mu r) \geq$ $\text{Arg}(\exp(ih_2) - \mu r)$ when m is odd; $h_1 + h_2 < m\pi, h_2 > 0,$ for any m .
$E_3^1(h_1) := \mu^{-1} + r \exp[-h_1, h_1],$ $E_3^2(h_2) := \mu^{-1} + r \exp[-ih_2, ih_2] \exp(i\pi m)$	$h_1 > 0, m\pi > h_2 > 0$

where the slots E_s^1, E_s^2 are defined in Table 3. The slots are invariant with respect to the involution Ξ and do not intersect each other as well as the boundary of the annulus $m \cdot \beta$.

To understand the interrelation of introduced constructions it is very useful to imagine how the pants $\mathcal{PB}1$ are transformed to the pants of fashion $\mathcal{Q} = \mathcal{B}23$ and the latter—to the pair of pants $\mathcal{PB}21$ or $\mathcal{PB}22$.

4.2 The Main Theorem

Theorem 4 *When $\lambda \neq 1, 3$ the Hölder’s antisymmetric eigenfunctions of PS-3 integral equation for the case $\mathcal{Q} = \mathcal{A}, \mathcal{B}1, \mathcal{B}21, \mathcal{B}22, \mathcal{B}23$ are in one to one correspondence with the pairs of pants² $\mathcal{PQ}(\lambda, h_1, h_2|m_1..)$ conformally equivalent to the pants (9) associated to the functional parameter of integral equation.*

Let the function $p(y)$ conformally maps the pair of pants $\mathcal{P}(R_3)$ to the pants $\mathcal{PQ}(\lambda, h_1, h_2|m_1..)$ and respects the colours of the boundary ovals, then up to proportionality

$$u(x) = \begin{cases} \sqrt{\frac{(y - y_1)(y - y_2)}{p'(y^+)p'(y^-)}} \frac{p(y^+) - p(y^-)}{w(y)}, & x \in [-1, 1] \setminus [a_1, a_2], \\ \sqrt{(y - y_1)(y - y_2)} \frac{\text{Im } p(y^+)}{w(y)|p'(y^+)|}, & x \in [-1, 1] \cap [a_1, a_2]. \end{cases} \tag{48}$$

Here $y := R_3(x), y^\pm := y \pm i0$. For the fashion $\mathcal{Q} = \mathcal{A}_1, y_1 = \bar{y}_2$ is the inner critical point of the function $p(y)$; for other fashions \mathcal{Q} real y_1 and y_2 are boundary critical points of the function $p(y)$.

The proof of the main theorem for the cases $\mathcal{A}, \mathcal{B}1$ is given in Section 6 and for the case $\mathcal{B}2$ —in Section 7.

4.3 Corollaries

The representation of eigenfunction (48) cannot be called explicit in the usual sense, since it comprises a transcendent function $p(y)$. We show that nevertheless the representation allows us to understand the following properties of the solutions.

1. *The “antisymmetric” part of the spectrum is always a subset of $[1, 3]$; for the equations of types $\mathcal{A}, \mathcal{B}1$ this part of the spectrum always lies in $[1, 2] \cup \{3\}$.*
2. *Every $\lambda \in (1, 3)$ is the eigenvalue for infinitely many equations PS-3.*

²For the case \mathcal{A} there are three stable and two unstable pants fashions $\mathcal{PA}_*(...)$

Proof Any of the constructed pants may be conformally mapped to the standard form: the sphere with three real slots. Now we can apply the procedure of the Section 2.5 and get the functional parameter $R_3(x)$ such that the associated pair of pants is conformally equivalent to the pants we started from.

3. *Eigenfunction $u(x)$ related to the pants $\mathcal{PQ}(\dots|m_1, m_2)$ has exactly $m_1 + m_2 + 1$ zeroes on the segment $[-1, 1]$ when $\mathcal{Q} = \mathcal{A}, \mathcal{B}1$.*

Proof According to the formula (48), the number of zeroes of eigenfunction $u(x)$ is equal to the number of points $y \in [-1, 1]$ where $p(y^+) = p(y^-)$. This number in turn is equal to the number of solutions of the inclusion

$$S(y) := \text{Arg}[p(y^-) - \mu^{-1}] - \text{Arg}[p(y^+) - \mu^{-1}] \in 2\pi\mathbb{Z}, \quad y \in [-1, 1]. \tag{49}$$

Let the point $p(y)$ goes m times around the circle C when its argument y travels along the banks of $[-1, 1]$. Integer m is naturally related to the integer parameters of pants $\mathcal{PQ}(\dots)$. The function $S(y)$ strictly increases from 0 to $2\pi m$ on the segment $[-1, 1]$, therefore the inclusion (49) has exactly $m + 1$ solutions on the mentioned segment. \square

4. *The mechanism for arising the discrete spectrum of the integral equation is explained. Sewing annuli down to the pants $\mathcal{PQ}(\lambda, h_1, h_2|\dots)$ one changes the conformal structure of the latter. To return to the conformal structure specified by $\mathcal{P}(R_3)$ we have to change the real parameters of the pants, one of them is the spectral parameter λ .*

In a sense, the eigenvalue problem (1) is reduced to the solution of three equations for three unknown numbers. These equations relate moduli of given pants $\mathcal{P}(R_3)$ to the moduli of membrane with real parameters λ, h_1, h_2 and extra discreet parameters.

5 Auxiliary Constructions

The combinatorial analysis of the arising projective structure $p(y)$ is based on two constructions we describe below.

Let $p(y)$ be a holomorphic map from a Riemann surface \mathcal{M} with a boundary to the sphere and the selected boundary component $(\partial\mathcal{M})_*$ is mapped to a circle. The reflection principle allows us to holomorphically continue $p(y)$ through this selected component to the double of \mathcal{M} . Therefore we can talk of the critical points of $p(y)$ on $(\partial\mathcal{M})_*$. When the argument y passes through a simple critical point, the value $p(y)$ reverses the direction of its movement on the circle. So there should be even number of critical points (counted with multiplicities) on the selected boundary component.

5.1 Construction 1 (No Boundary Critical Points)

Suppose that $p(y)$ has no critical points on the selected component of $\partial\mathcal{M}$ which is mapped to the boundary of the unitary disc

$$\mathbb{U} := \{p \in \mathbb{C} : |p| \leq 1\}. \tag{50}$$

We define the mapping from a disjoint union $\mathcal{M} \sqcup \mathbb{U}$ to a sphere:

$$\tilde{p}(y) := \begin{cases} p(y), & y \in \mathcal{M}, \\ y^{-d}, & y \in \mathbb{U}, \end{cases} \tag{51}$$

where integer $d \neq 0$ is the degree of the mapping $p : (\partial\mathcal{M})_* \rightarrow \partial\mathbb{U}$, d is positive (negative) if a small annular vicinity of the selected boundary component is mapped to the interior (exterior) of the unit disc. We also call d the *winding number* of $p(y)$ on the boundary oval $(\partial\mathcal{M})_*$.

Now we fill in the hole in \mathcal{M} by the unit disc, identifying the points of $(\partial\mathcal{M})_*$ and the points of $\partial\mathbb{U}$ with the same value of \tilde{p} (there are $|d|$ ways to do so). The holomorphic mapping $\tilde{p}(y)$ of the new Riemann surface $\mathcal{M} \cup \mathbb{U}$ to the sphere will have exactly one additional critical point of multiplicity $|d| - 1$ at the center of the glued disc.

5.2 Construction 2 (Two Boundary Critical Points)

Let again $p(y)$ be a holomorphic mapping of a bounded Riemann surface \mathcal{M} to the sphere with selected boundary component $(\partial\mathcal{M})_*$ being mapped to the boundary of the unit disc \mathbb{U} . Now the mapping $p(y)$ has two simple critical points on the selected boundary component (the case of coinciding critical values is not excluded). Those two points (Fig. 6) divide the oval $(\partial\mathcal{M})_*$ into two segments. We are going to modify the Riemann surface \mathcal{M} , sewing down one segment of $(\partial\mathcal{M})_*$ to the other and filling the remaining hole (if any) with the patch \mathbb{U} .

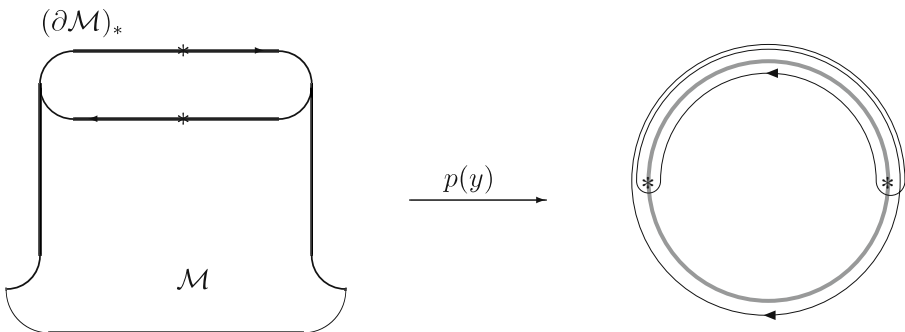


Fig. 6 Mapping of the boundary component $(\partial\mathcal{M})_*$ with two simple critical points $*$ on it and the degree $d = -1$

Again, we define the mapping from the disjoint union $\mathcal{M} \sqcup \mathbb{U}$ to the sphere by the formula (51) where integer d is the degree of the mapping $p : (\partial\mathcal{M})_* \rightarrow \partial\mathbb{U}$. In other words, $2\pi d$ is the increment of $\arg p(y)$ when the point y goes around the selected boundary oval in the positive direction.

We glue one segment of $(\partial\mathcal{M})_*$ to a part of the other, identifying the points of the boundary oval equidistant in the metric $|dp|$ from (any) chosen boundary critical point. If $d = 0$, the hole disappears. Otherwise we identify the remnant of $(\partial\mathcal{M})_*$ with the boundary of \mathbb{U} , gluing points with the same value of $\tilde{p}(y)$ as shown in the Fig. 7a.

The holomorphic mapping $\tilde{p}(y)$ of the modified Riemann surface to the sphere will have no additional critical points when $d = 0$. When $d \neq 0$ one or two additional critical point arise: one of multiplicity $|d| - 1$ at the center of the artificially attached disc and a simple critical point the place of the old boundary critical point other than chosen in the previous paragraph.

Remark The application of Constructions 1 and 2 to a given function $p(y)$ mapping boundary component of the surface \mathcal{M} to the circle contains an arbitrary element—linear fractional function mapping the given circle to the standard one, $\partial\mathbb{U}$. Changing this element we can (a) arbitrary move the additional critical value of \tilde{p} within appropriate disc and (b) change the sign of d . The choice of the additional critical value will simplify the arising combinatorial analysis and we always assume w.l.o.g. that $d \geq 0$.

6 Proof for the Cases $\mathcal{A}, \mathcal{B}1$

6.1 Eigenfunction Gives Pair of Pants

We already know that every antisymmetric eigenfunction of integral equation PS-3 generates the mapping $p(y)$ from the pants $\mathcal{P}(R_3)$ to the sphere. The boundary ovals of the pants are mapped to three circles specified in Theorem 3 and the function $p(y)$ may have either (a) no critical points, (b) one simple critical point inside the pants, (c) two boundary simple critical points or (d)

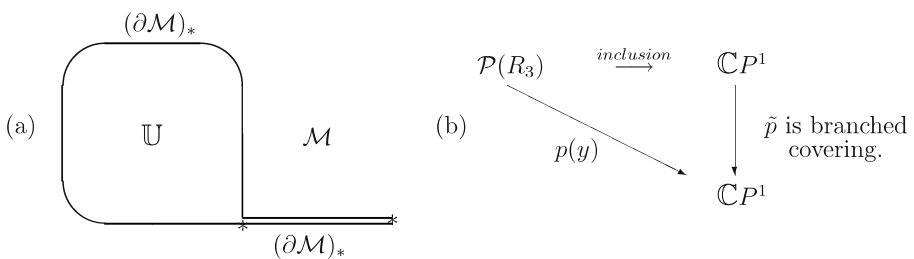


Fig. 7 (a) Filling in the hole bounded by $(\partial\mathcal{M})_*$ (b) Splitting of the mapping $p(y)$

one double critical point on the boundary. The first two possibilities will be considered in Section 6.1.1 and the other two—in the Section 6.1.2.

6.1.1 No Critical Points on the Boundary of Pants

Branched Covering of a Sphere Suppose that the point $p(y)$ winds around the corresponding circle d_r, d_g and d_b times when the argument y runs around the ‘red’, ‘green’ and ‘blue’ boundary component of $\mathcal{P}(R_3)$ respectively. We can apply the construction of Section 5.1 and glue three discs, $\mathbb{U}_r, \mathbb{U}_g, \mathbb{U}_b$ to the holes of the pants. Essentially, we have split our mapping $p(y)$ —see the commutative diagram on the Fig. 7b. The holomorphic mapping \tilde{p} has three or four ramification points, three of them are in the artificially glued discs and the fourth (if any) is inherited from the projective structure.

Applying the Riemann–Hurwitz formula we get:

$$\begin{aligned} d_r + d_g + d_b &= 2N, & p \text{ is branched,} \\ d_r + d_g + d_b &= 2N + 1, & p \text{ is unbranched,} \end{aligned} \quad N := \deg \tilde{p}. \quad (52)$$

Intersection of Circles

Lemma 7 *In case A the required projective structure $p(y)$ with a critical point inside the pants may exist only if the spectral parameter $1 < \lambda < 2$ (i.e. when the circle C does not intersect two other circles $\varepsilon^{\pm 1}\hat{\mathbb{R}}$). The structure without branching does not exist for any λ .*

Proof

1. We know that the point 0 lies in the intersection of two circles: $\varepsilon\hat{\mathbb{R}}$ and $\varepsilon^2\hat{\mathbb{R}}$. The total number $\#\{\tilde{p}^{-1}(0)\}$ of the pre-images of this points (counting the multiplicities) is N and cannot be less than $d_b + d_g$ —the number of pre-images on the blue and green boundary oval of the pants. Comparing this to (52) we get $d_r \geq N$ which is only possible when

$$d_r = d_g + d_b = N. \quad (53)$$

Assuming that the circle C intersects any of the circles $\varepsilon^{\pm 1}\hat{\mathbb{R}}$ we repeat the above argument for the intersection point and arrive at the conclusion $d_b = d_r + d_g = N$ or $d_g = d_r + d_b = N$ incompatible with already established (53).

2. For the unbranched structure $p(y)$ the established inequalities $d_b + d_g \leq N$ and $d_r \leq N$ contradict the Riemann-Hurwitz formula (52). □

The above arguments may be applied to the case $\mathcal{B}1$ as well. Taking into account that the circles C and $\hat{\mathbb{R}}$ always intersect we arrive at

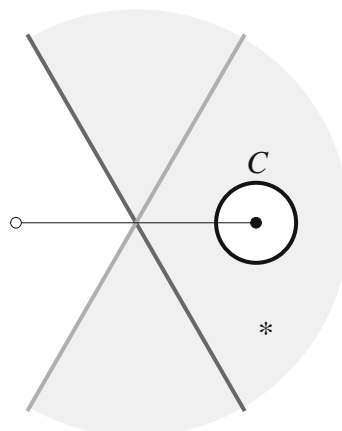
Lemma 8 *In case B1 the mapping $p(y)$ (if any) will have a boundary critical point.*

Image of Pants Let us investigate where the artificially glued discs in case \mathcal{A} are mapped to. Suppose for instance that the disc \mathbb{U}_r is mapped to the exterior of the circle C . The point 0 will be covered then at least $d_r + d_g + d_b = 2N$ times which is impossible. The discs \mathbb{U}_g and \mathbb{U}_b are mapped to the left of the lines $\varepsilon\mathbb{R}$ and $\varepsilon^2\mathbb{R}$ respectively, otherwise points from the interior of the circle C will be covered more that N times. The image of the pair of pants $\mathcal{P}(R_3)$ is shown on the Fig. 8.

We use the ambiguity in the construction of gluing the discs to the pants and require that the critical values of \tilde{p} in the discs $\mathbb{U}_g, \mathbb{U}_b$ coincide. Now the branched covering \tilde{p} has only three different branch points shown as \bullet, \circ and $*$ on the Fig. 8. The branching type at \bullet is the cycle of length N ; at the point \circ there are cycles of lengths d_g and d_b ; and the branch point $*$ is simple. The coverings with three branch points are called Belyi maps and are described by certain graphs known as Grothendieck’s “*Dessins d’Enfants*”. In our case the *dessin* is the lifting of the segment connecting white and black branch points: $\Gamma := \tilde{p}^{-1}[\bullet, \circ]$.

Combinatorial Analysis of Dessins There is exactly one critical point of \tilde{p} over the branch point $*$. Hence, the compliment to the graph Γ on the upper sphere of the diagram on the Fig. 7b contains exactly one cell mapped $2 - 1$ to the lower sphere. All the rest components of the compliment are mapped $1 - 1$. Two types of cells are shown in the Fig. 9a and b, the lifting of the red circle is not shown to simplify the pictures. The branch point $* =: h_1 + ih_2$ should lie in the intersection of two annuli α and $\bar{\alpha}$ otherwise the discs $\mathbb{U}_g, \mathbb{U}_b$ glued to different boundary components of our pants will intersect: the hypothetical case when the branch point of $p(y)$ belongs to one annulus but does not belong to the other is shown in the Fig. 9c.

Fig. 8 Shaded area is the image of pants in case \mathcal{A} , index $d_b \neq 0$



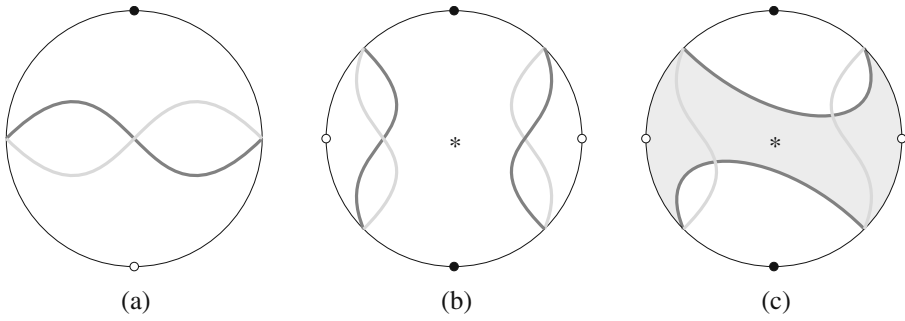


Fig. 9 (a) Simple cell ($N - 2$ copies) (b) Double cell (1 copy) (c) Impossible double cell

The cells from the Fig. 9a, b may be assembled in a unique way shown in the Fig. 10. The pants are colored in white, three artificially sewn discs are shaded. Essentially this picture shows us how to sew together the patches bounded by our three circles $C, \varepsilon^{\pm 1}\hat{\mathbb{R}}$ to get the pants conformally equivalent to $\mathcal{P}(R_3)$. As a result of the surgery procedure we get the pants $\mathcal{PA}_1(\lambda, h_1, h_2|d_g, d_b)$. Changing the superscript of the projective structure $p^{\pm}(y)$ gives us the change of sign for the eigenfunction $u(x)$ and the reflection of the pants $\mathcal{PA}_1(\dots)$ in the unit circle $\partial\mathbb{U}$. This is why we consider only the pants with $|h_1 + ih_2| \geq 1$.

6.1.2 Boundary Critical Points

First of all we consider the stable case of two simple critical points on the boundary oval. At the moment we do not know the color of this oval and we use the ‘nicknames’ {1, 2, 3} for the set of colours {r, g, b} so that the critical points will be on the oval 3.

Branched Covering of the Sphere The usage of both constructions from Section 5 allows us to include the pants $\mathcal{P}(R_3)$ to the sphere attaching two discs \mathbb{U}_1 and \mathbb{U}_2 to the first two ovals, collapsing the boundary of the third oval and

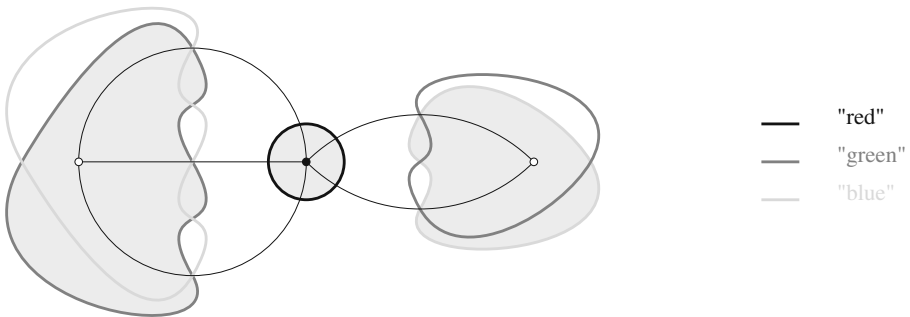


Fig. 10 Dessin for $d_g = 3, d_b = 2$; the pre-image of the branch point $*$ is at infinity

sewing in the third disc \mathbb{U}_3 if necessary. Nonnegative winding numbers arising in those constructions we denote as d_1, d_2, d_3 respectively.

We arrive at the branched covering \tilde{p} of the diagram on the Fig. 7b. This mapping has either two, three or four critical points. Two of them are in the centers of the discs $\mathbb{U}_1, \mathbb{U}_2$; another one or two points arise only when $d_3 \neq 0$ —the center of \mathbb{U}_3 and one of the boundary critical points of the mapping $p(y)$. The multiplicities of those critical points are respectively $d_1 - 1, d_2 - 1, d_3 - 1, 1$. Riemann-Hurwitz formula for this covering reads

$$d_1 + d_2 + d_3 = 2N, \quad N := \deg \tilde{p}. \tag{54}$$

Lemma 9 *The images of the ovals 1 and 2 do not intersect.*

Proof Suppose the inverse is true and a point Pt lies in the intersection of images of the first two ovals. Then $N \geq \# \tilde{p}^{-1}(Pt) \geq d_1 + d_2$. Any of the critical points from the third oval has at least $d_3 + 1 \leq N$ pre-images counting multiplicities. The last two inequalities contradict (54). \square

Corollaries

1. *In case A the critical points of $p(y)$ lie either on the blue or on the green boundary of pants. (Two circles $\varepsilon^{\pm 1} \hat{\mathbb{R}}$ intersect)*
2. *In case B1 the critical points of $p(y)$ lie on the blue boundary of pants. (Two circles C and $\hat{\mathbb{R}}$ intersect)*
3. *In both cases the required function may only exist when $\mu \in (\frac{1}{2}, 1)$, or equivalently $\lambda \in (1, 2)$. (Otherwise the circles C and $\varepsilon^{\pm 1} \hat{\mathbb{R}}$ intersect)
To save space, further proof will be given for the case A only when both critical points lie on the blue oval. The omitted cases require no extra technique. Now the notations $\mathbb{U}_r, \mathbb{U}_g, \mathbb{U}_b, d_r, d_g, d_b$ have the obvious meaning.*

Image of Pants

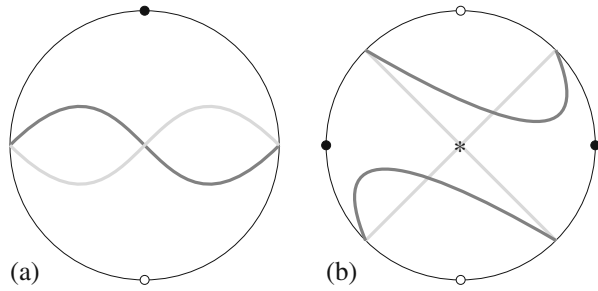
Lemma 10 *The image $p(\mathcal{P}(R_3))$ of the pants is the union $\alpha \cup \bar{\alpha}$ when $d_b \neq 0$ or the annulus α when $d_b = 0$.*

Proof Setting $Pt = 0$ in the proof of Lemma 9 we establish the equalities

$$d_g + d_b = d_r = N.$$

Now, repeating the arguments of the same title paragraph of the Section 6.1.1 we conclude that the disc $\tilde{p}(\mathbb{U}_r)$ fills the interior of C , the disc \mathbb{U}_g is mapped to the left of the line $\varepsilon \mathbb{R}$ and the disc \mathbb{U}_b (if any) is mapped to the left of $\varepsilon^2 \mathbb{R}$. So the sector $\{\frac{2\pi}{3} \leq \arg p \leq \frac{4\pi}{3}\}$ is covered $d_g + d_b = N$ times by the artificially inserted discs. The disc \mathbb{U}_g covers the half-plane to the left of the line $\varepsilon \mathbb{R}$ exactly d_g times, the latter number is N when $d_b = 0$. \square

Fig. 11 (a) Simple cell ($N - 2$ copies) (b) Double cell (1 copy)



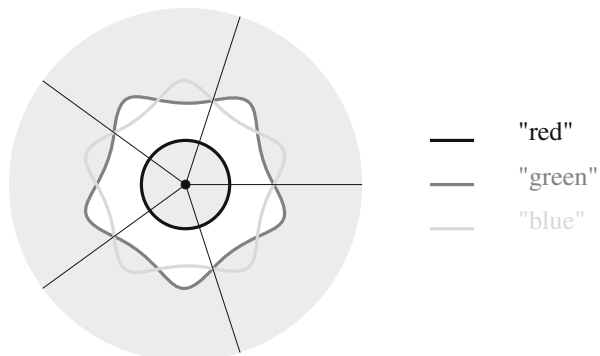
Corollary Both critical values of $p(y)$ lie on the ray $-\varepsilon^2(0, \infty)$.

Dessin d'Enfants Again, we put the critical values of \tilde{p} in the discs $\mathbb{U}_g, \mathbb{U}_b$ to the same point \circ (see Fig. 8). The only difference from the Section 6.1.1: now the inherited from the pants branch point $*$ (if $d_b \neq 0$) lies on the ray $-\varepsilon^2(0, \infty)$. We introduce the Grothendieck's *Dessin* as the lifting of the segment connecting white and black branch points: $\Gamma := \tilde{p}^{-1}[\bullet, \circ]$. The compliment to Γ is composed of cells shown in the Fig. 11. In the assembly the double cell may be used only once and only when $d_b \neq 0$.

Given the winding numbers d_g, d_b , the cells from the Fig. 11a, b may be attached to each other in a unique way. When $d_b \neq 0$ the *Dessin* Γ has the same combinatorial structure as in Fig. 10. Of course, one has to replace the old cells by those shown in Fig. 11. Shown in the Fig. 12 is the assembly of cells for $d_b = 0, d_g = 5$. The pants are colored in white, two artificially inserted discs are shaded. As a result of the surgery procedure we get the pants $\mathcal{P}\mathcal{A}_2(\lambda, h_1, h_2 | d_g, d_b)$ with positive reals h_1, h_2 determined by the critical values of $p(y)$. To discern the pair of pants $\mathcal{P}\mathcal{A}_2(\dots)$ from its reflection in the unit circle we consider the restriction $h_1 h_2 \geq 1$.

Junction of critical points To study the remaining case when the boundary critical points of projective structure merge, one has to apply the limit case of

Fig. 12 Degenerate Dessin for $d_g = 5, d_b = 0$; the pre-image of the branch point \circ is at infinity



the Construction 2. In this way one arrives at the unstable membranes \mathcal{PA}_{12} and \mathcal{PA}_{13} . To save space we omit the details.

6.2 Pair of Pants Corresponds to Eigenfunction

Let the pair of pants (9) associated to the functional parameter $R_3(x)$ of the type $Q = A, B1$ integral equation be conformally equivalent to the pants $\mathcal{PQ}(\lambda, \dots)$. This exactly means that there exists a conformal mapping $p(y)$ from $\mathcal{P}(R_3)$ to $\mathcal{PQ}(\lambda, \dots)$ respecting the colors of the boundary ovals. This mapping is unique since the conformal self-mapping of pants keeping all boundary ovals invariant is trivial. The mapping $p(y)$ has one simple critical point inside the pants (for the membrane $\mathcal{PA}_1(\dots)$) or two simple boundary points (for $\mathcal{PA}_2(\dots), \mathcal{PA}_3(\dots), \mathcal{PB1}(\dots)$) or a double boundary critical point (for $\mathcal{PA}_{12}(\dots), \mathcal{PA}_{13}(\dots)$). Moreover, $p(y)$ maps the boundary components of $\mathcal{P}(R_3)$ to the circles specified by Theorem 3. Hence, given $p(y)$ one can consecutively restore: two projective structures $p^\pm(y)$, the solution $W(y)$ of Riemann monodromy problem and the eigenfunction $u(x)$. Combining the formulae (44), (36) we obtain the top of the reconstruction formulae in (48).

7 Proof for the Case $\mathcal{B}2$

7.1 Eigenfunction Gives Pair of Pants

Any antisymmetric eigenfunction of the integral equation $PS-3$ generates the mapping $p(y)$ from the pants $\mathcal{P}(R_3)$ to the sphere. The principal difference of this case from the one considered in Section 6 lies in the two-valuedness of the function $p(y)$ in the pants. To reflect this phenomenon we consider the two sheeted unbranched cover $\mathcal{P}_2 \rightarrow \mathcal{P}(R_3)$ with trivial monodromy around the green boundary oval. This new surface is a sphere with four holes, each boundary inherits the color of the oval it covers—see Fig. 13a. The mapping

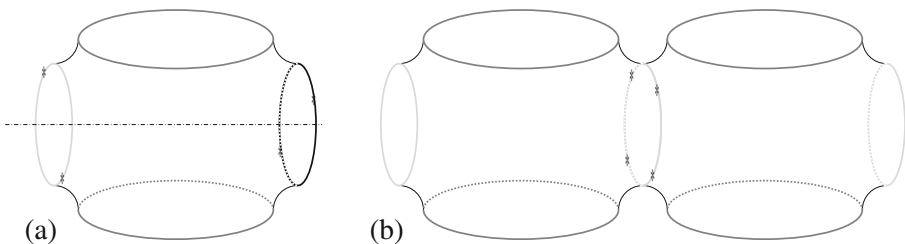


Fig. 13 (a) The surface \mathcal{P}_2 is the double cover of pants \mathcal{P} ; (b) \mathcal{P}_4 is the reflection of \mathcal{P}_2 in the blue boundary oval

$p(y)$ is lifted to the single-valued mapping $p_2 : \mathcal{P}_2 \rightarrow \mathbb{C}P^1$ satisfying the equivariance condition:

$$p_2 \Xi = \chi(\mathbf{DD}_1)p_2, \tag{55}$$

where Ξ is the cover transformation (change of sheets) of \mathcal{P}_2 , represented as the rotation by 180° around the horizontal axis on Fig. 13a.

Now we can complete the proof of the Lemma 6.

Suppose that there exists the required function $p_2(y)$ in the case $\mathcal{B}21$ and $\mu > 1$. We show that all possible locations of the critical points of this function lead to the contradiction: **(a)** p_2 has no boundary critical points; **(b)** all critical points lie on the green ovals of \mathcal{P}_2 ; **(c)** p_2 has at least one critical point on a blue oval.

- (a)** We use the Construction 1 and attach four discs to the surface \mathcal{P}_2 . For the arising ramified covering \tilde{p}_2 the Riemann-Hurwitz formula reads

$$\begin{aligned} 2d_g + d_b + d'_b &= 2N, & p \text{ is branched,} \\ 2d_g + d_b + d'_b &= 2N + 2, & p \text{ is unbranched,} \end{aligned} \quad N := \deg \tilde{p}_2,$$

where d_g is the winding number (degree) of $p_2(y)$ on each of the green ovals; d_b and d'_b are the winding numbers for two blue ovals of the surface \mathcal{P}_2 . The point $0 \in \hat{\mathbb{R}} \cap \varepsilon \hat{\mathbb{R}}$ is covered at least $d_g + d_b + d'_b \leq N$ times. This agrees the previous formula only if $d_g \geq N$. But now $d_b = d'_b = 0$ which is impossible.

- (b)** Now each of two green ovals has two boundary critical points of $p_2(y)$. We use both Constructions and eliminate all holes in \mathcal{P}_2 attaching two discs to the blue ovals and possibly two more discs to the green ovals of the surface. The Riemann-Hurwitz formula for the arising ramified covering \tilde{p}_2 reads

$$2d_g + d_b + d'_b = 2N, \quad N := \deg \tilde{p}_2,$$

where $d_g \geq 0$ is the degree of $p(y)$ for each of the green ovals of \mathcal{P}_2 . Further argument is exactly as in the previous paragraph.

- (c)** We claim that in this case there are exactly four critical points of p_2 on a blue oval of the surface \mathcal{P}_2 . Indeed, given a critical point Pt , ΞPt is also a critical point because of the equivariance (55). When $\mu > 1$, the mapping $\chi(\mathbf{DD}_1)$ conserves the orientation of the real axis. This means that those two critical points are of the same type (say, local maxima of the real value p_2). Hence, Pt and ΞPt are separated by the critical points of the opposite type (local minima in our case). There cannot be more that four boundary critical points of the function p_2 on the double cover of pants $\mathcal{P}(R_3)$, so we have listed them all.

Let us consider the *double* of the surface \mathcal{P}_2 and cut it along all boundary ovals of \mathcal{P}_2 , but the blue oval containing all critical point of $p_2(y)$. This new surface, \mathcal{P}_4 , is a sphere with six holes shown in the Fig. 13b, four boundary ovals are green and two are blue. The reflection principle allows to continue

analytically $p_2(y)$ to the mapping $p_4(y)$ of the entire surface \mathcal{P}_4 to the sphere. This continuation has four inner critical points and no boundary critical points. It maps both blue ovals to $\hat{\mathbb{R}}$ and four green ovals to the circles $\varepsilon^{\pm 1}\hat{\mathbb{R}}$, $\chi(\mathbf{DD}_1)\varepsilon^{\pm 1}\hat{\mathbb{R}}$. The usage of Construction 1 allows to fill in all the holes of \mathcal{P}_4 . The Riemann-Hurwitz formula for the arising ramified covering \tilde{p}_4 reads

$$2d_g + d_b = N, \quad N := \deg \tilde{p}_4,$$

where the numbers d_g, d_b have the obvious meaning. The point 0 is covered at least $2d_g + 2d_b > N$ times which is impossible.

The location of the critical points of the mapping $p_2(y)$ is given by the following lemma.

Lemma 11 *The mapping $p_2(y)$ has exactly two boundary critical points on each of the non-green ovals of the surface \mathcal{P}_2 .*

Proof The mapping $\chi(\mathbf{DD}_1)$ changes the orientation of the circles C and $\hat{\mathbb{R}}$, when $\mu \in (0, 1)$. When the point y runs along the blue or red oval of \mathcal{P}_2 , the value $p_2(y)$ changes the orientation of its motion at least twice due to (55). This means that the argument y comes through at least two boundary critical points. Since the mapping $p(y)$ has at most two boundary critical points in pants, the lifted mapping $p_2(y)$ has at most four in the double cover of pants. \square

Branched covering of the sphere The mapping $p_2(y)$ from \mathcal{P}_2 to the sphere has equal winding numbers $d = d_g$ on both green ovals. The degree of $p_2(y)$ on each of non-green ovals equals zero. Both statements are simple consequences of the equivariance condition (55). Applying Constructions 1 and 2 to the mapping p_2 defined on \mathcal{P}_2 , we get a ramified covering \tilde{p}_2 with two critical points, both of multiplicity $d_g - 1$.

Image of the Surface The Riemann-Hurwitz formula for the ramified covering \tilde{p}_2 reads $d_g = N := \deg \tilde{p}_2$. It is easily seen that two discs attached to the green ovals of \mathcal{P}_2 are mapped to the left of the line $\varepsilon \mathbb{R}$ and to the interior of the circle $\chi(\mathbf{DD}_1) \varepsilon \hat{\mathbb{R}}$. Therefore, the surface \mathcal{P}_2 is conformally equivalent to the closure of the annulus $d_g \cdot \beta$ with two slots in it.

The involution Ξ of \mathcal{P}_2 (the interchange of sheets) induces the involution of the multisheeted annulus. The latter involution is the lifting of $\chi(\mathbf{DD}_1)$ to $d_g \cdot \beta$ and is given by the formula (47). The slots of $d_g \cdot \beta$ are invariant with respect to Ξ and therefore pass through the fixed points $\mu^{-1} + r$ and $\mu^{-1} + r \exp i\pi m$ of the involution. The red slots are projected to the circle C , the blue slots are projected to the real line. Given in Table 3 inequalities for the parameters h_1, h_2 specifying the endpoints of the slots allow us to relate any given antisymmetric eigenfunction to exactly one picture.

A by-product of the explicit description of the image of the pants is the following

Lemma 12 *In antisymmetric case B2 two structures $p^\pm(y)$ are different when $\lambda \neq 3$.*

Proof Suppose the opposite is true, that is

$$p(y)\overline{p(\bar{y})} \equiv 1 \tag{56}$$

for meromorphic function $p(y)$ satisfying the conditions of Theorem 3.

In case B21 the value $p(a) \in \mathbb{R}$ when $a \in \{a_1, a_2\}$ is the endpoint of the blue slot. From (56) it immediately follows that $p(a) = \pm 1$. But the image of pants $p\mathcal{P}(R_3) = \beta$ avoids both points ± 1 .

In case B22 the value $p(a \pm i0) \in C = \{p = \chi(\mathbf{DD}_1)\bar{p}\}$ when $a \in \{a_1, a_2\}$ is the endpoint of the red slot. From (56) and the jump relationship (46) on $[a_1, a_2]$ it follows that $p(a \pm i0) = \pm 1$. Again, the image of pants $p(\mathcal{P})$ avoids both points ± 1 .

In case B23 any of the above two arguments is applicable. □

Corollary *In case B2 any eigenvalue corresponds to no more than one anti-symmetric eigenfunction.*

Proof Suppose, there are two linearly independent antisymmetric eigenfunctions of the integral equation (1) with common eigenvalue. They generate two couples of meromorphic functions in the slit sphere $\mathcal{P}(R_3) \setminus [-1, 1]$, say p^\pm, p_0^\pm . The analytic continuation of those four functions gives four projective structures on the riemann surface M with common monodromy determined by the eigenvalue. From Lemma 12 it follows that no two of the four structures are identical and therefore (see the second part of the proof of the Theorem 2) all four values $p^\pm(y), p_0^\pm(y)$, are different at any point y .

We consider the following differential form on the Riemann surface M :

$$\omega := dp^+ \left(\frac{1}{p^+ - p_0^+} - \frac{1}{p^+ - p_0^-} \right).$$

This form ω is the infinitesimal form of the cross ratio and it is invariant under the same linear-fractional transformations of three functions p_0^\pm, p^+ . Therefore ω is well defined on the entire Riemann surface M . Using local coordinates on M , it's easy to check that the form is holomorphic and $(\omega) = D(p^+)$. Any holomorphic differential on the genus 2 surface has two zeroes which are interchanged by the hyperelliptic involution of M . According to Lemma 11, the branching divisor of $p_1(y)$ is different as it has a branchpoint on each of non-green ovals of the pants \mathcal{P} . □

7.2 Pair of Pants Corresponds to Eigenfunction

Let the pair of pants $\mathcal{PB}2s(\lambda, h_1, h_2|m)$ be conformally equivalent to the pair of pants $\mathcal{P}(R_3)$ associated to type B2s, $s = 1, 2, 3$, integral equation. This

exactly means that there exists respecting the colors of the boundary ovals equivariant conformal mapping $p_2(y)$ from the double cover $\mathcal{P}_2(R_3)$ of pants to the closure of the multisheeted annulus $m \cdot \beta$ with two slots $E_5^1(h_1)$ and $E_5^2(h_2)$ in it. We represent the double cover $\mathcal{P}_2(R_3)$ as two copies of pants $\mathcal{P}(R_3)$ cut along the segment $[-1, 1] \cap [a_1, a_2]$ and attached one to the other. The restriction of $p_2(y)$ to one of such copies gives the function $p(y)$ satisfying all the assumptions of the Theorem 3. The antisymmetric eigenfunction of the integral equation now may be reconstructed via the known procedure which gives the formulae (48). Moreover, from Lemma 12 we have learned that the invariant $J_0 \neq 0$ for antisymmetric solutions in the case $\mathcal{B}2$. So we can use the alternative formula (41) to reconstruct the eigenfunction $u(x)$ when $x \in [-1, 1] \setminus [a_1, a_2]$. On the remaining part of the segment $[-1, 1]$ we can use along with (48) the other formula:

$$u(x) = \frac{\text{Im } p(y^+)}{|p(y^+) - \mu|^2 + 1 - \mu^2}, \quad y^+ := R_3(x + i0), \quad x \in [-1, 1] \cap [a_1, a_2].$$

The only nuisance here consists in possible non-uniqueness of the mapping $p(y)$. Indeed, when two of the boundary ovals of pants have the same color (blue in case $\mathcal{B}21$ or red in case $\mathcal{B}22$), the pants may admit conformal involution interchanging the ovals of the same color. Such pants fill in a codimension one manifold in the corresponding moduli space. The Corollary to Lemma 12 nevertheless guarantees the uniqueness of the antisymmetric eigenfunction for the given membrane $\mathcal{PB}2s$: the composition of $p(y)$ with the conformal automorphism of pants coincides with either $p(y)$ or its antisymmetrization $1/\overline{p(\bar{y})}$.

8 Conclusion

The geometric and combinatorial analysis of the spectral problem for the Poincare-Steklov integral equation is given in this paper. Another powerful approach to the study of integral equations is the theory of operators. It is always useful to compare two different viewpoints on the same subject.

The study of the spectral problem (1) based on the theory of singular integral operators was carried out in [1, 2]. The following results were obtained for general smooth coordinate changes $R(x)$ provided the non-degeneracy condition (2) holds: (i) The spectrum is discrete; the eigenvalues are positive and converge to $\lambda = 1$; (ii) $\sum_{\lambda \in Sp} |\lambda - 1|^2 < \infty$ (a constructive estimate in terms of $R(x)$ may be given); (iii) The eigenfunctions $u(x)$ make up an orthogonal (with respect to a special scalar product) basis in the Sobolev space $H_{oo}^{1/2}(I)$.

The geometric approach was first applied to the $PS - 2$ integral equations with $R(x) = x + (2C)^{-1}(x^2 - 1)$, the parameter $C > 1$. The complete set of

eigen-values and functions from the above Sobolev space has been explicitly found [3]:

$$u_n(x) = \sin \left[\frac{n\pi}{K'} \int_1^{(C+x)/(C-1)} (s^2 - 1)^{-1/2} (1 - k^2 s^2)^{-1/2} ds \right], \quad (57)$$

$$\lambda_n = 1 + 1/\cosh 2\pi \tau n, \quad n = 1, 2, \dots,$$

where $\tau = K/K'$ is the ratio of the complete elliptic integrals of modulus $k = (C - 1)/(C + 1)$. All Poincare-Steklov equations with the eigenfunctions expressed in terms of elliptic functions were listed in [10]. The next natural step was to study equations (1) with a rational degree 3 functions $R(x)$ [11]. In this paper we show that all the eigenfunctions of PS-3 equations are split into two classes (symmetric/antisymmetric) with respect to the symmetries of the underlying geometric structures and we give the representation for all antisymmetric eigenfunctions (further analysis shows that this class is larger than the remaining one). The representation is given by an explicit formula (48) which contains a transcendental function $p(y)$ conformally mapping some explicitly constructed pair of pants to the standard form. Of course, this answer is less explicit than e.g. formula (57). The immediate consequences of this formula listed in Section 4.3 include: the exact locus of the spectrum for the family of equations, the oscillatory behaviour of the higher eigenfunctions; the mechanism for the emergence of the separate eigenvalues. Further study of the eigenvalues and eigenfunctions is now reduced to the problems of geometric function theory. Say, the explicit asymptotical formulae for the solutions may be written in the case when the conformal mapping of the pants to the standard three-slit domain is known approximately (short slots, small holes etc.).

It seems that the results of the mentioned two approaches are complementary. Operator theory may be applied in a rather general situation and it gives rather general answers. The usage of geometrical analysis is more restricted (e.g. may be applied to rational parameters $R(x)$) and more difficult. But if we are lucky, this analysis may give us the best of the answers—the explicit formulae for the solutions. The author hopes that some of the techniques used in this paper may be helpful for the study of other integral equations with rational low degree kernels.

References

1. Bogatyrev, A.B.: The discrete spectrum of the problem with a pair of Poincare-Steklov operators. *Doklady RAS* **358**(3) (1998)
2. Bogatyrev, A.B.: The spectral properties of Poincare-Steklov operators. PhD Diss., INM RAS, Moscow (1996)
3. Bogatyrev, A.B.: A geometric method for solving a series of integral PS equations. *Math. Notes* **63**(3), 302–310 (1998)
4. Poincare, H.: *Analyse des travaux scientifiques de Henri Poincare*. *Acta Math.* **38**, 3–135 (1921)

5. Gunning, R.C.: Special coordinate coverings of Riemann surfaces. *Math. Ann.* **170**, 67–86 (1967)
6. Tyurin, A.N.: On the periods of quadratic differentials. *Russ. Math. Surv.* **33**(6) (1978)
7. Gallo, D., Kapovich, M., Marden, A.: The monodromy groups of Schwarzian equations on closed Riemann surfaces. *Ann. Math. (2)* **151**(2), 625–704 (2000) See also arXiv, [math.CV/9511213](https://arxiv.org/abs/math.CV/9511213)
8. Hejhal, D.A.: Monodromy groups and linearly polymorphic functions. *Acta Math.* **135**, 1–55 (1975)
9. Mandelbaum, R.: Branched structures and affine and projective bundles on Riemann surfaces. *Trans. AMS* **183**, 37–58 (1973)
10. Bogatyrev, A.B.: Poincare-Steklov integral equations and the Riemann monodromy problem. *Funct. Anal. Appl.* **34**(2), 9–22 (2000)
11. Bogatyrev, A.B.: PS-3 integral equations and projective structures on Riemann surfaces. *Sb. Math.* **192**(4), 479–514 (2001)